Rec. Trav. Chim. Pays-Bas **109**, 537–551 (1990) 0165–0513/90/11537–15$4.25

On the mechanism of epoxidation of alkenes with hypochlorite, catalysed by manganese(III) tetraarylporphyrins†

A. W. van der Made‡ *, R. J. M. Nolte# and W. Drenth

Department of Organic Chemistry, Rijksuniversiteit Utrecht, Padualaan 8, 3584 CH Utrecht, The Netherlands

(Received May 10th, 1990)

Abstract. A detailed mechanistic study of the epoxidation of alkenes by the cytochrome-P-450 model sodium hypochlorite/manganese(III) tetraarylporphyrin is presented. From the zero-order rate dependence on alkene concentration and low-temperature-trapping experiments with the hydrogen-atom donor 1,1-diphenyl-2-picrylhydrazine (DPPH) it is concluded that the formation of the active $[(\mathbf{P})MnO]^+$ species from a (**P**)MnOCl complex is the rate-determining step of the reaction. The trapping experiments also show that the reverse reaction is possible. Pyridine or imidazole derivatives as axial ligands accelerate the rate-determining step by electron donation. Imidazoles, however, are destroyed under the reaction conditions. A general base function of pyridine or imidazole derivatives is excluded on the basis of experiments with porphyrin catalysts containing covalently bound pyridine. Large amounts of pyridine or imidazole retard the epoxidation reaction by blocking both sides of the catalyst, and thus preventing the hypochlorite anion to coordinate. In spite of the zero-order-in-alkene concentration, different alkenes are expoxidized at different rates. This is explained by the occurrence of dimerization phenomena, *i.e.*, a reaction of the $[(\mathbf{P})MnO]^+$ species with Mn^{III}, which eventually leads to catalyst destruction. Electron-rich substrates effectively prevent this destruction. In the case of sterically hindered catalysts, *i.e.*, catalysts bearing bulky substituents on the *ortho* positions of the phenyl rings, no dimerization occurs. With this class of catalysts, however, reaction rates are influenced by steric interactions between catalyst and substrate. Electron-withdrawing substituents on the 4-positions of the phenyl rings of the catalyst increase the epoxidation rate. This is a result of increased electrophilicity of the $[(\mathbf{P})MnO]^+$ species and decreased electron density at the *meso* positions making the catalyst less susceptible to destruction. Lowering the pH of the aqueous phase from 13.5 to 12.7 increases the rate of epoxidation, because, at lower pH, a neutral HCl molecule must be expelled from a $[(\mathbf{P})MnHOCl]^+$ complex instead of a chloride anion, in order to form the active species. Alcohols increase the reaction rate by providing better solvation of the leaving group (Cl^- or HCl). Aldehydes and ketones, which are formed as by-products in epoxidation, accelerate the reaction in the case of sterically not hindered catalysts. These compounds rapidly trap the active species, thus preventing unfavourable dimerization processes occurring. A carbonyl oxide species is produced, which in turn acts as an active epoxidizing agent. The reaction between the $[(\mathbf{P})MnO]^+$ species and an alkene is likely to proceed via a non-concerted process by interaction of the LUMO of the active species with the HOMO of the alkene in an asymmetrical way. With this mechanism, the formation of *trans*-epoxides from *cis*-alkenes as well as the formation of aldehydes and ketones as by-products are easily explained. Pyridines increase the stereoselectivity of the reaction by pulling the metal centre into the porphyrin plane. This creates increased steric hindrance to rotation of the oxo-substrate intermediate.

Introduction**

The discovery that simple metalloporphyrins in combination with a single-oxygen donor can mimic cytochrome-P-450-type oxidation reactions, provided a powerful impetus to study the mechanism of these models and their possible applications as epoxidizing and hydroxylating agents. The most successful model systems consist of a manganese(III) or iron(III) tetraarylporphyrin [(**P**)MnX and (**P**)FeX, respectively] and a single-oxygen donor, such as iodosylbenzene (C_6H_5IO)[1-7], pentafluoroiodosylbenzene (C_6F_5IO)[8-11], hydrogen peroxide (H_2O_2)[12-15], *tert*-butyl hydroperoxide (*t*-BuOOH)[12-15], 3-chloroperoxybenzoic acid (3-CPBA)[16-19], 4-cyano-*N*,*N*-dimethylaniline *N*-oxide (4-

† From the thesis by *A. W. van der Made*, Utrecht, 1988.

‡ Address of correspondence: Dr. *A. W. van der Made*, Koninklijke/Shell Laboratorium Amsterdam, P.O. Box 3003, 1003 AA Amsterdam, The Netherlands.

\# Present address: Department of Organic Chemistry, Katholieke Universiteit Nijmegen, Toernooiveld, 6525 ED Nijmegen, The Netherlands.

** Porphyrins are indexed in *Chem. Abstr.* as 21*H*,23*H*-porphines.

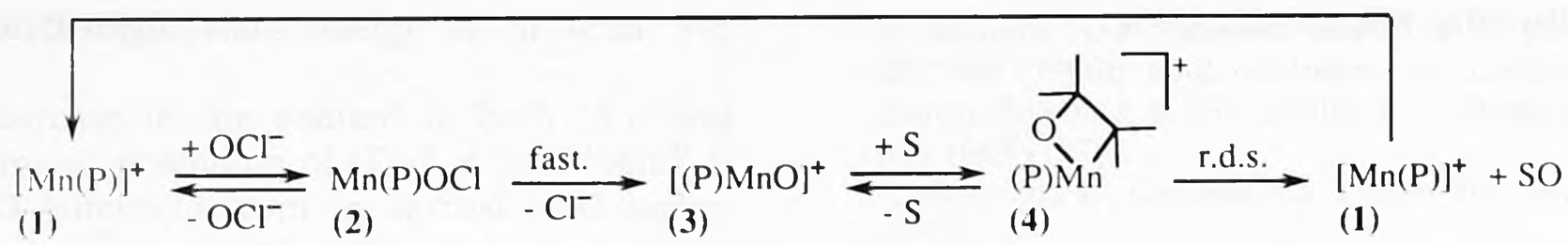

Scheme 1. Catalytic cycle according to Collman *et al.*

-CNDMANO)[20-22], and hypochlorite (OCl^-)[23-43]. In all systems, an oxo–metal species is the active epoxidizing agent. For 4-CNDMANO-[21,22], C_6F_5IO-[11], and *t*-BuOOH-[12] -based systems, it has been shown that the formation of this oxo species is the rate-determining step (r.d.s.). For the hypochlorite system, two opinions exist. *Collman* et al. found that, at high substrate concentrations, the reaction rate is zero order in substrate[29,30]. Different alkenes, however, were epoxidized at different rates. Therefore, according to those authors, the alkene must be involved in the r.d.s. This apparently contrasting behaviour was explained by the formation of a metallaoxetane intermediate which decomposes in a r.d.s. to epoxide and Mn(**P**)X. According to *Collman* et al., this view was supported by the observed Michaelis–Menten kinetics (see Scheme 1).

Our group has published several kinetic studies on the hypochlorite system, from which we concluded that, under our conditions, the formation of the active oxo species is the r.d.s.[33,34,36,37,41]. In agreement with *Collman* et al., we also found that the epoxidation reaction is zero order in alkene and that different alkenes are epoxidized at different rates. We explained this behaviour by the mechanism depicted in Scheme 2. Once formed in a r.d.s., the active species $[(\mathbf{P})MnO]^+$ **3** will react with one of the substrates to yield epoxide and $Mn^{III}(\mathbf{P})X$, or with $Mn^{III}(\mathbf{P})X$ to form a $[(\mathbf{P})Mn^{IV}–O–Mn^{IV}(\mathbf{P})]^{2+}$ μ-oxo dimer **6**. Dimer formation retards the epoxidation reaction because part of the catalyst becomes tied up in a catalytically inactive form. A reactive substrate competes more successfully with $Mn^{III}(\mathbf{P})X$ for the oxo species than an unreactive one. As a consequence, there is less dimer formation and a higher epoxidation rate. In order to be able to present a more complete picture, we have extended our investigation of the hypochlorite-based epoxidation system.

Results and discussion

The various steps of the catalytic cycle will be discussed in detail.

Step 1. (P)MnCl → (P)MnOCl

The epoxidation of alkenes by Mn(**P**)Cl and sodium hypochlorite is performed in a two-phase water/dichloromethane system under phase transfer conditions. Reaction conditions, *e.g.*, phase-transfer catalyst concentration (> 0.001 $mol \cdot dm^{-3}$, preferably 0.005 $mol \cdot dm^{-3}$), stirring speed (1100 rpm), and hypochlorite concentration (> 0.2 $mol \cdot dm^{-3}$, preferably 0.4 $mol \cdot dm^{-3}$) were chosen in such a manner that the transportation of the OCl^- ion from the aqueous to the organic phase is not rate limiting. From a Lineweaver–Burk plot of the reciprocal of the epoxidation rate *versus* the reciprocal of $[OCl^-]$ a K_m value of $9.36 \cdot 10^{-2}$ $mol \cdot dm^{-3}$ is obtained (reaction conditions: see experimental)[44]. Assuming that the decomposition of (**P**)MnOCl to $[(\mathbf{P})MnO]^+$ is slow, this K_m value indicates that $[(\mathbf{P})Mn]^+$ has a higher affinity for OCl^- than for Cl^- (see Eqn. 1).

$$Mn(\mathbf{P})Cl + OCl^- \rightleftharpoons Mn(\mathbf{P})OCl + Cl^- \quad (1)$$

Under standard two-phase conditions, the reaction mixture rapidly turns brown once stirring has started.

In a previous publication[45], we mentioned that the addition of triethylbenzylammonium hypochlorite, TEBAOCl, to Mn($T_{2,4,6}$triMePP)Cl or Mn($T_{2,6}$diClPP)Cl in CH_2Cl_2 at −50 °C produces a similar, instantaneous colour change from green to brown. For the species thus generated, we postulated the structure (**P**)MnOCl **2**[45,49-51,53,55,56]. For abbreviated names of catalysts see Note 52.

Step 2. (P)MnOCl → [(P)MnO]+ + Cl−

a. Trapping experiments. Trapping experiments on the active species with 1,1-diphenyl-2-picrylhydrazine (DPPH) at low temperature in CH_2Cl_2 permitted the following conclusions[57]:

(i) The overall rate-determining step of the catalytic cycle is the decomposition of (**P**)MnOCl to the active species $[(\mathbf{P})MnO]^+$ and Cl^-.
(ii) The reverse reaction is possible[54].
(iii) Pyridines increase the rate of formation of $[(\mathbf{P})MnO]^+$ from (**P**)MnOCl (see also next Section).

b. Influence of axial ligands. Addition of pyridine or its derivatives to the two-phase system leads to an increased epoxidation rate, as is shown in Table I[25,27,34]. A Hammett treatment of the rate data of substituted pyridines (4-CH_3, 3-CH_3, 4-H, 3-Br, and 4-CN) gives a ρ value of −1.00 ± 0.05 for Mn(TPP)Cl. This indicates that electron-donating groups increase the reaction rate relative to unsubstituted pyridine. Electron donation by axially coordinated pyridine facilitates the rate-determining expulsion of

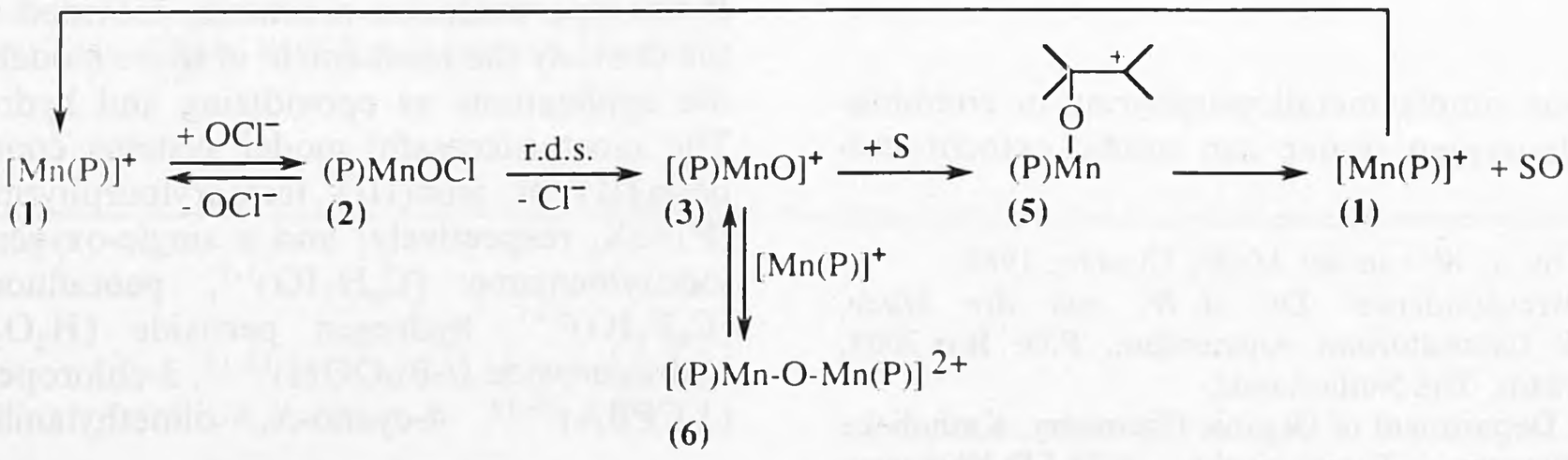

Scheme 2. Catalytic cycle as proposed by our group.

the Cl^- ion from the (**P**)MnOCl complex to form the active species. The necessity of pyridine coordination to the metal centre is demonstrated by the lower rates observed for the sterically hindered pyridines, 2,6-dimethylpyridine and 2,6-di-*tert*-butylpyridine, notwithstanding their electron-donating substituents. Experiments with catalysts **P4**, **P8**, and **P11** (see Figure 1) support this view. In these

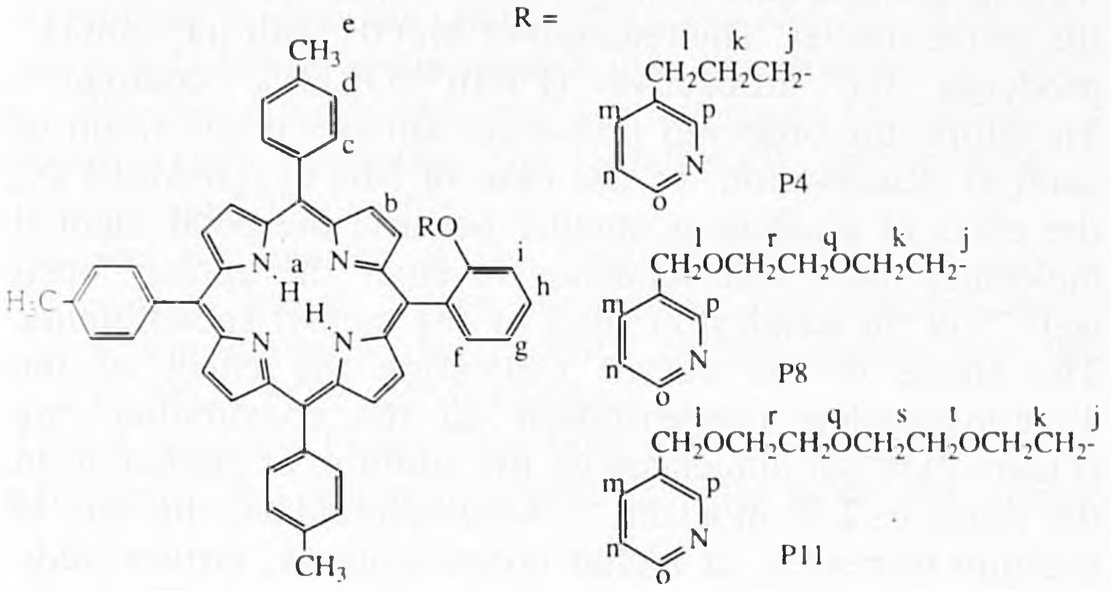

*Fig. 1. Structure and adopted lettering for porphyrins **P4**, **P8**, and **P11**.*

compounds, the ease of coordination of the covalently attached pyridine molecule to the manganese centre decreases with increasing spacer length, as a result of steric crowding. This trend is reflected by the observed epoxidation rates **P4** > **P8** > **P11** ≈ Mn(TPP)Cl in the absence of pyridine (see Table I).

Table I Epoxidation rate[a], of cyclohexene for various porphyrin catalysts in the presence of substituted pyridines.

Catalyst	Additive		
	None	4-Methylpyridine	2,6-Dimethylpyridine[b]
Mn(TPP)X	0.42	10.9	0.42
P4	3.43	13.7	3.40
P8	1.84	12.8	1.90
P11	0.50	9.9	0.50

[a] Rate × 10^5/(mol · dm^{-3} · s^{-1}). [b] Identical rates were obtained with 2,6-di-*tert*-butylpyridine.

A possible role of pyridine as a general base catalyst is excluded by experiments with catalysts **P4**, **P8** and **P11**. Addition of 2,6-dimethylpyridine, which is incapable of binding to the manganese centre because of steric hindrance[57] but should still be able to act as a general base, has no influence on the epoxidation rate displayed by these catalysts. Only one molecule of pyridine coordinated to the manganese atom is, therefore, required.

In the range 0–2.75 mol · dm^{-3}, 4-methylpyridine increases the epoxidation rate (see Figure 2). Larger amounts have a deleterious effect. A similar but less pronounced trend is observed for the sterically hindered Mn($T_{2,4,6}$triMePP)Cl. At high concentrations, pyridine decreases the reaction rate by occupying both axial coordination sites of manganese(III) to form a bis(pyridine) complex[57]. This complex has no catalytic activity because the OCl^- ion cannot coordinate anymore.

Collman et al. reported that the addition of imidazoles, especially *N*-(4-acetylphenyl)imidazole (NAcPhIm), enhances the epoxidation rate[28]. However, we have observed

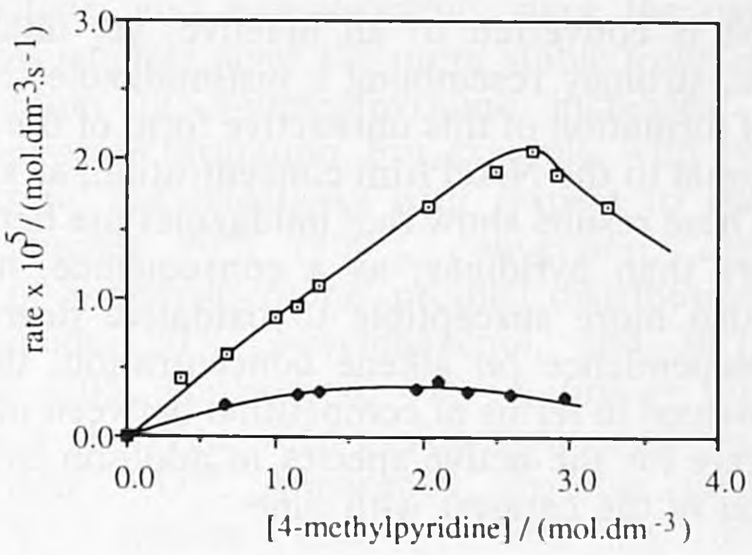

Fig. 2. Rate of cyclohexene epoxidation as a function of the 4-methylpyridine concentration for Mn(TPP)X (□) and for Mn($T_{2,4,6}$triMePP)X (◆). Standard conditions.

several differences compared to pyridine-based systems:

(i) For NAcPhIm, the ligand effect is stronger but highly compressed with respect to concentration; an almost linear increase in epoxidation rate from 0–0.49 mol · dm^{-3} NAcPhIm and a decrease above this concentration. Small amounts of imidazole and *N*-methylimidazole (> 0.05 mol · dm^{-3}) completely block the reaction by forming bis(imidazole) complexes (see also Ref. 57).

(ii) The order in substrate changes from zero (pyridine) to one (NAcPhIm) (see Figure 3).

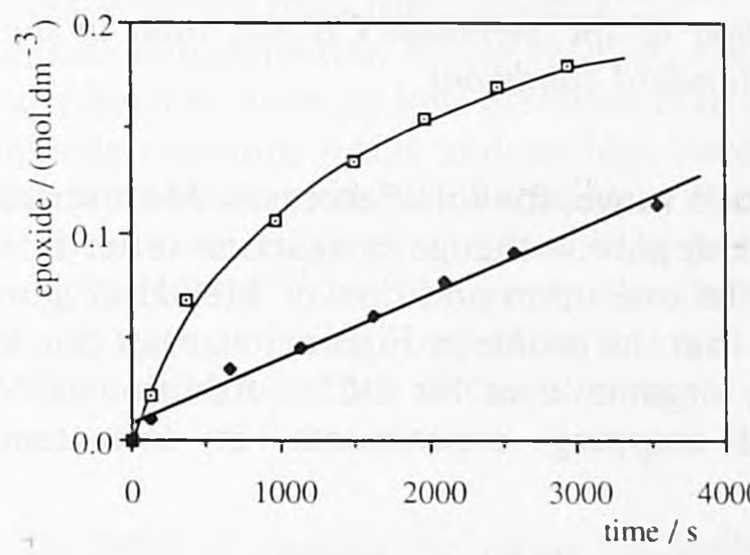

Fig. 3. Cyclohexene epoxidation in the presence of NAcPhIm (□) or 4-methylpyridine (◆) as axial ligands. Conditions: [NAcPhIm] 0.062 mol · dm^{-3}, [4-methylpyridine] 0.062 mol · dm^{-3}, (Mn(TPP)X] 6.1 · 10^{-4} mol · dm^{-3}.

(iii) In contrast to pyridines, imidazoles are oxidized under the reaction conditions[58].

(iv) The maximum number of turnovers decreases with increasing NAcPhIm concentration (see Figure 4).

The decreasing efficiency of the catalyst is not due to catalyst destruction. We found that, under these conditions,

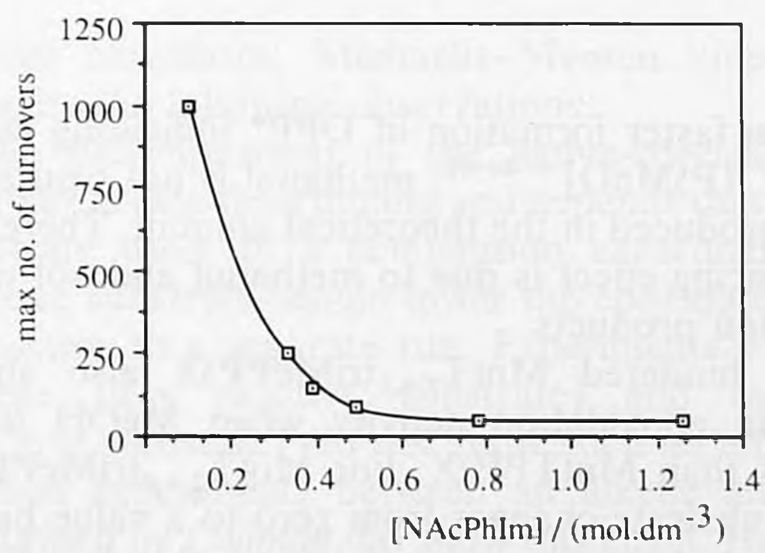

Fig. 4. Turnover numbers as a function of the NAcPhIm concentration. Standard conditions.

the catalyst is converted to an inactive, yet unidentified Mn^{III} state, strongly resembling a bis(imidazole) complex. The rate of formation of this unreactive form of the catalyst is proportional to the NAcPhIm concentration, as shown in Figure 4. These results show that imidazoles are better electron donors than pyridines; as a consequence, however, they are also more susceptible to oxidative degradation. The rate dependence on alkene concentration, therefore, can be explained in terms of competition between imidazole and substrate for the active species in addition to gradual deactivation of the catalyst with time.

c. Influence of methanol. Addition of methanol increases the epoxidation rate within the range 0–0.3 $MeOH/CH_2Cl_2$ v/v for Mn(TP**P**)X (Figure 5, see also Ref. 36). Above this

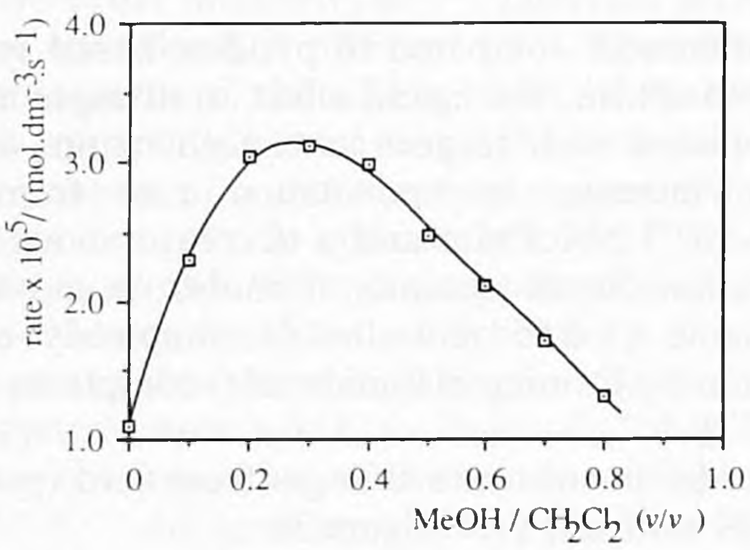

*Fig. 5. Initial rate of cyclohexene epoxidation by Mn(TP**P**)X as a function of the methanol/CH_2Cl_2 ratio in the reaction mixture. Standard conditions.*

concentration range, the rate decreases. Most striking, however, is the apparent change in reaction order in substrate from zero to one upon addition of MeOH (Figure 6). We confirmed that the profile in Figure 5 was not due to starvation of the organic layer for OCl^-. Addition of MeOH in the DPPH-trapping experiments at low temperature

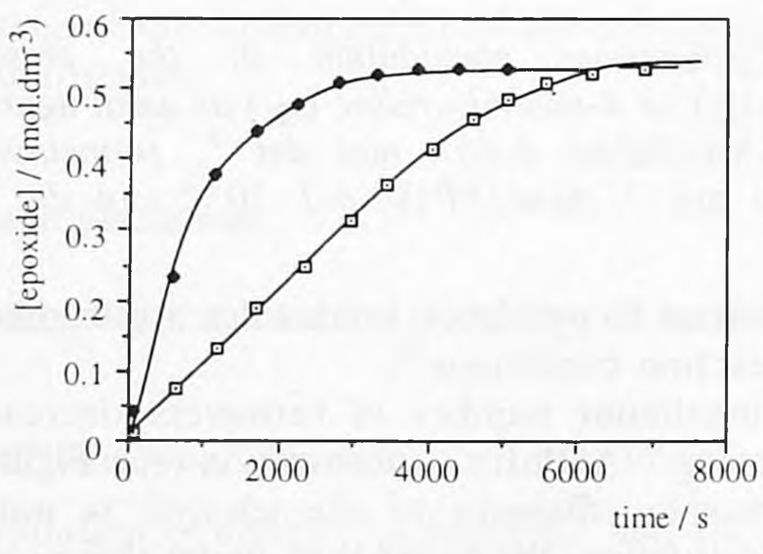

*Fig. 6. Cyclohexene epoxidation by Mn(TP**P**)X in the presence (◆) and the absence (□) of methanol. Standard conditions.*

resulted in faster formation of DPP• indicating faster formation of $[(\mathbf{P})MnO]^+$ [46-48]; methanol is not oxidized since DPP• is produced in the theoretical amount. Therefore, the rate-enhancing effect is due to methanol and not to one of its oxidation products.

Sterically hindered Mn($T_{2,4,6}$triMeP**P**)X also shows an increase in epoxidation activity when MeOH is added, albeit less than Mn(TP**P**)X. For Mn($T_{2,4,6}$triMeP**P**)X, the order in substrate changes from zero to a value between 0 and 1. Ethanol, 1-propanol and 1-butanol induced an effect similar to but less pronounced than that of methanol.

Alcohols enhance the epoxidation rate by increasing the polarity of the organic medium. In this way, the rate-determining cleavage of the O–Cl bond in the (**P**)MnOCl complex **2** is facilitated by better solvation of the chloride anion. The change in kinetics would suggest that, upon addition of an alcohol, the reaction of the active species **3** with substrate instead of its formation becomes rate determining[36]. Experiments in which the amount of methanol is varied, show that this is not true. When present in high concentration, alcohols successfully compete with the substrate for the active species. The reaction of MeOH with $[(\mathbf{P})MnO]^+$ produces the unreactive $(\mathbf{P})Mn^{IV}(OCH_3)_2$ complex[59]. Therefore, the observed first-order kinetics is the result of catalyst deactivation. In the case of Mn($T_{2,4,6}$triMeP**P**)X, the effect of alcohols is smaller because the polar alcohol molecules have little tendency to enter the apolar "open well"[42] of the catalyst created by the methyl substitutents. The shape of the curves expressing the effect of the 4-methylpyridine concentration on the epoxidation rate (Figure 2) is not influenced by the addition of methanol. In the range 0–2.75 $mol \cdot dm^{-3}$ 4-methylpyridine, the rate of reaction increases; at higher concentrations, further addition has a negative effect on the epoxidation rate. This indicates that the addition of methanol does not change the catalytic cycle.

d. Effect of pH. Recently, it was reported by *Montanari* et al. that lowering the pH of the aqueous phase from pH 13.5 to 9.5 had a beneficial effect on the epoxidation rate[39,60-62]. This effect was interpreted in terms of an acceleration of the rate-determining break-down of a cyclic metallaoxetane intermediate **4** (see Scheme 1), by an unknown mechanism. Since this explanation contrasted with our scheme (see Scheme 2) in which the formation of the active species $[(\mathbf{P})MnO]^+$ (**3**) from (**P**)MnOCl (**2**) is the rate-determining step, we decided to reinvestigate the "pH effect".

In an earlier publication[63], we have described the results of this investigation. On the basis of these results, we explain the rate-enhancing effect of lowering the pH as follows: At a lower pH, the $[(\mathbf{P})MnO]^+$ species will be formed more rapidly by expulsion of a neutral HCl molecule from a protonated $[(\mathbf{P})MnHOCl]^+$ species. This species can be formed by coordination of HOCl to Mn(**P**)X or by protonation of MnOCl. The latter possibility is most likely because, even at pH 10.0, a phase-transfer catalyst is needed. Since the protons act catalytically, only a small amount is required. This explains the sharp increase in epoxidation rate upon a moderate change in pH. Between pH 13.5 and 12.7, the reaction rate is first order in proton concentration for Mn(TP**P**)X. Low-temperature trapping experiments with DPPH (see *Step 2a*) support this view[57,63]. Addition of a HCl-containing DPPH solution in CH_2Cl_2 to a (**P**)MnOCl solution results in faster formation of DPP•. This indicates faster formation of $[(\mathbf{P})MnO]^+$ from (**P**)MnOCl.

Addition of methanol (*i.e.*, increasing the polarity of the organic phase, see *Step 2c*) also has a rate-enhancing effect at pH 10.0 as at pH 13.5; this as a result of increased solubility of HCl, which is released when the active species is formed (epoxidation rate without methanol $8.3 \cdot 10^{-5}$ $mol \cdot dm^{-3} \cdot s^{-1}$; with ethanol $15.0 \cdot 10^{-5}$ $mol \cdot dm^{-3} \cdot s^{-1}$). This similar behaviour of the system at pH values of 13.5 and 10.0 supports the view that, on lowering the pH, there is no major change in mechanism, *i.e.*, although the formation of $[(\mathbf{P})MnO]^+$ is accelerated, it still remains the rate-determining step.

Step 3. $[(\mathbf{P})MnO]^+ + \mathbf{S} \rightarrow [(\mathbf{P})Mn]^+ + \mathbf{SO}$

a. Mechanism. According to the overall reaction equation, the oxygen atom that is transferred to the alkene, originates

from the hypochlorite ion. Using an ^{18}O-labeled (**P**)MnOCl complex, we noted indeed ^{18}O incorporation in the epoxide. The extreme instability and reactivity of the oxo species prevented its thorough characterization by standard methods. We, therefore, performed *ab-initio* calculations to determine its structure and to explain its reactivity[64,65]. Our calculations on the model compound, oxo-manganese porphyrin chloride, revealed the following details:

(i) The structure of the active species in which the oxo moiety bridges the manganese atom and one of the pyrrole N atoms is more stable than the structure in which the oxo atom is attached to manganese exclusively.

(ii) For both structures, the closed-shell conformation is the most favourable.

(iii) The mechanism of the reaction between the active species and an alkene involves an asymmetrical interaction between the HOMO of the alkene and the LUMO of the active species.

This is shown in Figure 7 for both oxo structures. In chemical terms, this means electron transfer from the alkene

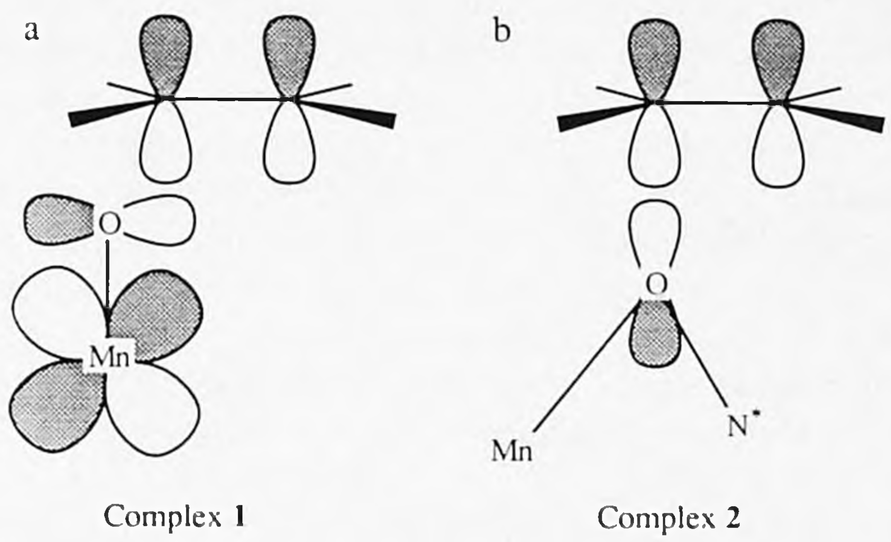

Complex 1 Complex 2

Fig. 7. Interaction between the HOMO of an alkene and the LUMO of the active species for (a) the "linear structure" and (b) the "inserted structure".

towards the oxo species. This transfer produces a carbocation. This is supported by experiments in which various 4-substituted styrenes are epoxidized[66]. Hammett treatment shows a good linear correlation of log(rate) *versus* σ^+ with ρ^+ values of -0.48 for Mn(TP**P**)Cl and -0.44 for Mn($T_{2,4,6}$triMeP**P**)Cl. Negative ρ^+ values point to the development of a positive charge on the α carbon atom of styrene in the transition state (the initial attack is on the β carbon)[67]. The almost similar ρ^+ values for Mn(TP**P**)Cl and Mn($T_{2,4,6}$triMeP**P**)Cl indicate that, for both catalysts, similar active species and transition states are involved.

In the carbocation, the alkene-double-bond character is lost and rotation in the direction of the most stable configurational isomer is possible. Steric interactions with the porphyrin ring will hinder this rotation. Support for this idea is given by *Groves*[2], who observed that substituents at the *ortho* positions of Mn(TP**P**)X increased the stereoselectivity of *cis*-stilbene epoxidation. A similar observation was made for Mn($T_{2,4,6}$triMeP**P**)X (see also Ref. 42). Steric interactions also depend on the position of the Mn atom with respect to the N_4 plane of the porphyrin. The closer the metal is to the centre of this plane, the more hindered the rotation in the intermediate will be. The increase in stereoselectivity of the epoxidation reaction upon addition of pyridine has been attributed to this effect, *i.e.*, the Mn atom is pulled into the N_4 plane by axially ligating pyridine[68]. Obviously, rotation will only occur if there is sufficient driving force towards the energetically more favourable product (*i.e.* $k_{epoxidation} < k_{rotation}$). This explains the pseudo-stereospecificity observed by *Collman*[30] for *trans*-2-methylstyrene, *trans*-2-octene, and *trans*-4-octene, since the oxidation of these *trans* isomers gives the more stable *trans* epoxides.

The addition of 4-methylpyridine increases selectivity towards epoxide formation. For example, with cyclohexene as substrate, the selectivity with respect to epoxide formation reaches 90% (100% conversion, 2 h). In the absence of 4-methylpyridine, product distribution becomes 40% epoxide, 30% 2-cyclohexenol, and 30% 2-cyclohexenone (50% conversion, 4 h). A similar product distribution is observed when cyclohexene is allowed to react with (**P**)$Mn^{IV}=O$[69]. Apparently, pyridine stabilizes the $[(P)MnO]^+$ species and prevents its decay into (**P**)Mn^{IV}=O, a process which has been observed in the related Mn($T_{2,4,6}$triMeP**P**)OH/3-CPBA system[17]. In this way, a higher rate and more selective epoxidation are observed[70].

b. Kinetic analysis. The kinetics of the reaction are conveniently determined by monitoring the substrate and epoxide concentrations as a function of time by gas chromatography. In earlier publications, both our group[33,34,36,37,41] and *Collman*'s group[28-30] reported a zero-order dependence in alkene up to 80% substrate conversion. Our present analysis, using many substrates and catalysts, reveals that the data only fit to a zero-order dependence up to 40% conversion. Since the first part of a first-order curve is often mistaken for a zero order, experiments were repeated at double substrate concentration (0.8 mol·dm^{-3}). Only a slight increase in epoxidation rate was opbserved (see Table II) indicating an order slightly higher than zero, but definitely disfavouring first-order kinetics.

More accurate determination of the reaction order in substrate is not feasible since, at low substrate concentrations, competing side reactions occur and, at high substrate concentrations, the reaction rate is influenced by the change in polarity of the system. In general, above 40% substrate conversion, the order in substrate gradually shifts to one. Therefore, all rate constants reported in this article are obtained from zero-order fits of the data up to 40% substrate conversion.

Table II The effect of doubling the alkene concentration on the epoxidation rate.

Catalyst	Substrate	Acceleration[a]
Mn(T_2ClP**P**)X	cyclopentene	1.39
	cyclooctene	1.10
Mn(T_2FP**P**)X	cyclopentene	1.27
	styrene	1.08
Mn($T_{2,4,6}$triMeP**P**)X	1-methylcyclohexene	1.25

[a] (Rate at 0.8 mol·dm^{-3} alkene)/(rate at 0.4 mol·dm^{-3} alkene). Theoretical value for zero order: 1; for first order: 2.

Under our conditions, Michaelis–Menten kinetics were ruled out by the following observations:

(i) If the decomposition of the active-species-substrate complex is rate-determining and depends on the type of substrate used, in a competition experiment, a less reactive substrate should lower the epoxidation rate of a reactive to a separate run. Experiments with cyclohexene (less reactive substrate) and cyclooctene (reactive substrate) did not show such an effect. Competition experiments between an alkene and styrene performed by *Collman* did show this effect. However, in our opinion, the use of styrene for this purpose may have been unfortunate (see *Step 3c*).

(ii) Saturation of the catalyst with substrate would lead to a build-up of an active-species-substrate complex since its decomposition is rate-determining. Our various attempts to observe such a complex (metalloxetane) were unsuccessful. Similarly, *Traylor*[9] failed to detect any metallaoxetane intermediate for the Fe(TpentaFPP)X/C_6F_5IO system, which was said to show Michaelis–Menten kinetics similar to the hypochlorite system[8]. The only transient species observed was a reversible formed *N*-alkylporphyrin. Kinetic analysis showed that, in this system, the formation of the active species, $(P^{\bullet+})Fe^{IV}=O$, is the rate-determining step[9,11]. Experiments by *Suslick* et al. on the Mn($T_{2,4,6}$triPhPP)/NAcPhIm/LiOCl system with conjugated dienes as substrates also do not support the presence of a metallaoxetane intermediate[43].

(iii) We found that the rate data for cyclohexene and Mn(TPP)Cl can be fitted to Michaelis–Menten kinetics with fair correlation (r 0.90) within the range 0.05–0.8 mol · dm^{-3} (apparent K_m 15 mol · dm^{-3}). Sterically hindered porphyrins with either electron-donating [Mn($T_{2,4,6}$triMePP)Cl] or electron-withdrawing [Mn(T_2ClPP)C] groups, however, showed lower K_m values (K_m 1.2 and 2.0 mol · dm^{-3}, respectively). This indicates that these catalysts would have a higher affinity for the substrate than Mn(TPP)Cl, an effect which cannot be rationalized in terms of formation of an active-species-substrate complex governed by steric or electronic effects. The high apparent K_m value indicates that Mn(TPP)Cl requires a fairly high substrate concentration to function properly. A high substrate concentration could decrease rate-retarding phenomena, *e.g.*, catalyst deactivation, which do not occur with sterically hindered catalysts *(vide infra)*.

As mentioned before, different substrates are epoxidized at different rates. Our explanation of this effect is that the alkene, depending on its reactivity, more or less successfully competes with Mn^{III} and Cl^- for the active $[(P)MnO]^+$ species[34,37]. The epoxidation rates for cyclohexene, cyclooctene, cyclopentene, 1-methylcyclohexene, *cis*-stilbene, and styrene are given in Table III. A comparison of these data with those obtained with peracetic acid[71] (see Table IV) points to the unique position of styrene as a substrate in the Mn(P)X/OCl^- system *(vide infra)*. With all catalysts, cyclopentene and cyclooctene are epoxidized faster than cyclohexene. It has been suggested[72-75] that the dominant enthalpy feature in establishing this order appears to be relief of torsional strain, with diminished bond-angle strain also playing an important role in cyclopentene.

Electronic effects also govern the reactivity of alkenes, as is revealed by experiments with various *para*-substituted styrenes *(vide supra)*. Electron-donating groups enhance the reactivity of the alkene, whereas electron-withdrawing groups decrease it. This is also illustrated by the higher reactivity of 1-methylcyclohexene as compared to cyclohexene in the case of Mn(TPP)Cl and Mn(T_2FPP)Cl. However, with sterically hindered catalysts [Mn($T_{2,4,6}$triMePP)X, Mn($T_{2,4,6}$triMeOPP)X], the rate-enhancing function of the CH_3 group of the substrate is counteracted by increased steric hindrance of the substrate, as is expressed by a lower rate of 1-methylcyclohexene relative to cyclohexene. Steric effects of substrates also become apparent in the epoxidation of *trans*-stilbene. In epoxidations with 3-CPBA in CH_2Cl_2 at room temperature *cis*- and *trans*-stilbene display equal reactivity. In the Mn(P)X/OCl^- system with sterically hindered catalysts, *trans*-stilbene is not epoxidized at all.

These results show that the reactivity of the alkene, *i.e.*, its ability to compete with Cl^- and Mn^{III}(P)X (in the case of a sterically not hindered porphyrin) for the active species, is influenced by electronic as well as steric factors. In most cases (styrene excluded), the rates for various alkenes differ in magnitude by a factor of about 3. At conversions up to 40%, the alkene is not involved in the r.d.s. at all, as is displayed by a zero order in alkene. At conversions greater than 40%, the alkene becomes involved in the r.d.s., as is expressed by the gradual change in reaction order in alkene. The tetraarylporphyrin ligand influences the epoxidation reaction not only sterically, but also electronically. The steric effect is indicated by the following experiments. For sterically not hindered catalysts (4-MeO, 4-Me, 4-F, 4-Cl, 4-NO_2, 4-NMe_2, 4-H) and aliphatic substrates, we observe, in the concentration range $0 < [Mn(P)X] < 4 \cdot 10^{-3}$ mol · dm^{-3}, an apparent decrease in reaction order in catalyst from one to zero with increasing catalyst concentration (Figure 8) (see also Ref. 4).

Table IV Relative reactivities of various alkenes with peracetic acid in acetic acid[a].

Substrate	Relative rate
ethene	1[b]
propene	25
cyclopentene	1000
cyclohexene	675
cyclooctene	900
styrene	60

[a] Taken from Ref. 71. [b] Rate at 25.8 °C $1.5 \cdot 10^{-4}$ dm^3 · mol^{-1} · s^{-1}.

Table III Epoxidation rates for various substrates with varous Mn(P)X catalyst under standard conditions.

Catalyst[d]	Epoxidation rates[a] for substrate[b]					
	CH	CO	CP	1-MCH	*cis*-Stilbene[c]	Styrene
Mn($T_{2,4,6}$triMeOPP)Cl	58	150	183	53	28	96
Mn(T_2ClPP)Cl	170	306	357	177	56	212
Mn(T_2FPP)Cl	169	458	569	212	78	283
Mn($T_{2,4,6}$triMePP)Cl	34	99	97	19	20	97
Mn(TPP)Cl	109	339	243	149	82	600
Mn($T_{2,6}$diClPP)Cl	13	–[e]	–[e]	–[e]	–[e]	–[e]

[a] Epoxidation rate/(10^{-6} · mol · dm^{-3} · s^{-1}). [b] CH = cyclohexene, CO = cyclooctene, CP = cyclopentene, 1-MCH = 1-methylcyclohexene. [c] At 5 °C. [d] Mn(T_2MePP)Cl, Mn(T_2MeOPP)Cl, and Mn(TpentaFPP)Cl are markedly destroyed under these reaction conditions. [e] Not determined.

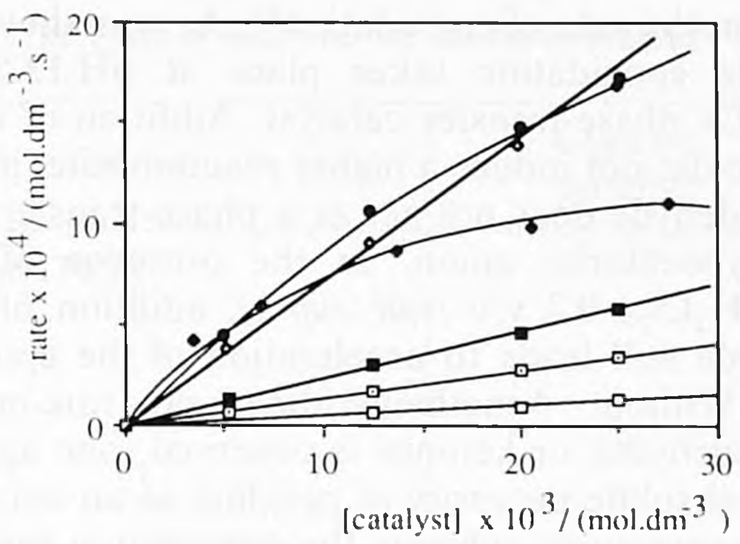

Fig. 8. Influence of the catalyst concentration on the epoxidation rate for Mn(TPP)X (◆), Mn($T_{2,4,6}$triMePP)X (■), Mn($T_{2,4,6}$triMeOPP)X (■), Mn(T_2ClPP)X (◊), Mn(T_2FPP)X (●), and Mn($T_{2,6}$diClPP)X (□). Other sterically not hindered catalysts. 4-MeO, 4-Me, 4-F, 4-NO_2, and 4-NMe_2 showed similar curves as Mn(TPP)X. Substrate cyclohexene, standard conditions.

Styrene shows an exceptional behaviour as the order in catalyst remains one over the entire concentration range $0 < \text{Mn(P)X} < 4 \cdot 10^{-3}$ mol · dm^{-3}. Over the same concentration range, with both aliphatic and aromatic alkenes, sterically hindered porphyrins (2,4,6-triMe, 2,4,6-triMeO, 2,6-diCl, 2-Cl, 2-F) constantly exhibit a first order behaviour (Figure 8). These suggest that the active [(P)MnO]$^+$ species reacts in two ways:

$$[(\mathbf{P})\text{MnO}]^+ + \text{alkene} \rightarrow [(\mathbf{P})\text{Mn}]^+ + \text{epoxide} \qquad (2)$$

$$[(\mathbf{P})\text{MnO}]^+ + [(\mathbf{P})\text{Mn}]^+ \rightleftarrows \mu\text{-oxo dimer} \rightarrow \text{destructed porphyrin} \qquad (3)$$

Reaction 3 is only significant with sterically not hindered porphyrins.

Under *Step 3c*, we will show that dimerization can be prevented by trapping the [(P)MnO]$^+$ or (P)MnOCl species with carbonyl compounds to form a carbonyl oxide, which, in turn, acts as a powerful epoxidation reagent. As a consequence of reaction 3, part of the total amount of such a porphyrin is tied up in the catalytically inactive μ-oxo dimer state. Because the formation of [(P)MnO]$^+$ is slow, a sterically not hindered catalyst is subject to increasing dimerization with increasing catalyst concentration. This is reflected by the apparent decrease in catalyst order from one to zero. *Hill* et al.[5,6] showed that dimer formation is a reversible process; a similar observation was made by *Spreer* et al.[48]. In both cases, the μ-oxo dimer was capable of reacting with alkenes, albeit with lower activity than the monomeric [(P)MnO]$^+$ species. This means that, under reaction conditions in our system, reversible dimer formation is likely. In the absence of substrate, the μ-oxo dimer decays destructively to Mn^{III}(P)X. In the presence of a reactive substrate (*e.g.*, cyclohexene), we found that for Mn(TPP)X no catalyst destruction takes place before 80% substrate conversion. With less reactive substrates (*e.g.*, propene, *trans*-stilbene), destruction already takes place in the initial stages of the reaction. Other catalysts, *e.g.*, the electron-rich sterically not hindered Mn(T_2OCH_3PP)X, Mn(T_4OCH_3PP)X, Mn(T_2CH_3PP)X, and Mn(T_4CH_3PP)X and the extremely electronegative Mn(TpentaFPP)X, have a limited stability even in the presence of highly reactive substrates (*e.g.*, styrene, *cis*-stilbene).

The electronic effect of the porphyrin ligand can be deduced from epoxidation experiments with a series of tetrakis-(*para*-substituted phenyl)porphyrins. *Para* substituents were chosen to eliminate any possible steric effect. A Hammett plot gives ρ values of 0.26 ± 0.09 and 0.32 ± 0.11 for cyclohexene and styrene, respectively (*r* 0.993) (see also Ref. 4). These values indicate that electron-donating substituents decrease and electron-withdrawing substituents increase the epoxidation rate. Electron withdrawal increases the electrophilicity of the [(P)MnO]$^+$ moiety, thus enhancing its reactivity towards the electron-rich double bond of a substrate. Too many electronegative groups, however, produce an ineffective catalyst since, in that case, the rate-determining formation of the active species from (P)MnOCl is very slow, as in the case of Mn($T_{2,6}$diClPP)Cl (see *Step 2a*).

The effect of the *para* substituents of the phenyl rings on the metal centre is clearly illustrated by electrochemical measurements. With cyclic voltammetry, the E^0 values for the $Mn^{III}(\mathbf{P})^+ \rightarrow Mn^{II}(\mathbf{P})$ reduction were determined. A plot of these data versus the 4σ value for the *para* substituent has a slope of 62 mV and a correlation coefficient *r* 0.98.

We may derive a rate equation using the following scheme:

$$(\mathbf{P})\text{MnOCl} \underset{k_{-2}}{\overset{k_2}{\rightleftharpoons}} [(\mathbf{P})\text{MnO}]^+ + \text{Cl}^-$$

$$[(\mathbf{P})\text{MnO}]^+ + \mathbf{S} \underset{k_{-3}}{\overset{k_3}{\rightleftharpoons}} [(\mathbf{P})\text{Mn}]^+ + \mathbf{SO}$$

S = substrate

Under conditions where dimerization is negligible, $d[(\mathbf{P})\text{MnO}]^+/dt = 0$, and k_{-3} is very small, the rate is:

$$v = \frac{k_2 \cdot [(\mathbf{P})\text{MnOCl}] \cdot k_3 \cdot [\mathbf{S}]}{k_{-2} \cdot [\text{Cl}^-] + k_3 \cdot [\mathbf{S}]}$$

If $k_3 \cdot [\mathbf{S}] \gg k_{-2} \cdot [\text{Cl}^-]$ then

$$v = k_2 \cdot [(\mathbf{P})\text{MnOCl}]$$

and a zero order in substrate is observed. If $k_3 \cdot [\mathbf{S}] \ll k_{-2} \cdot [\text{Cl}^-]$ then

$$v = \frac{k_2 \cdot [\text{MnOCl}] \cdot k_3 \cdot [\mathbf{S}]}{k_{-2} \cdot [\text{Cl}^-]}$$

In this case, the reaction rate becomes first order in substrate and has a reciprocal dependency on the $[\text{Cl}^-]$. Under the actual conditions, the order in substrate will be in between those extremes. In addition, it should be noted that the amount of Cl^- present in the organic phase will be fairly constant since the maximum amount of Cl^- is related to the amount of phase-transfer catalyst present in the organic phase.

c. Effect of carbonyl compounds. Styrene differs from other alkenes in the sense that *(i)* it is epoxidized very smoothly by Mn(TPP)X and *(ii)* in its presence, the order in catalyst is one over the concentration range $0–2.5 \cdot 10^{-3}$ mol · dm^{-3} Mn(TPP)X. The unique position of styrene is also reflected by the outcome of competition experiments with this substrate (Figure 9).

Addition of styrene to a solution of cyclohexene boosts the epoxidation rate of the latter compound and changes the kinetics, indicating that simple competition kinetics cannot be applied in this situation. We found that phenylacetaldehyde, which is produced as a by-product (≈20%) in styrene epoxidation, is the cause of the synergistic effect[41]. Addition of pure phenylacetaldehyde (0.136 mol · dm^{-3}) to a solution of cyclohexene gave a 4.1-fold

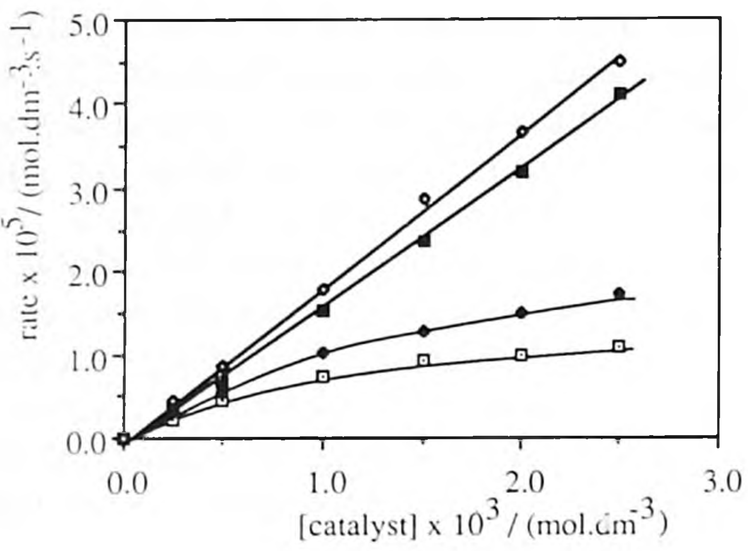

Fig. 9. The effect of styrene and aldehydes on the epoxidation of cyclohexene catalysed by Mn(TPP)X. Standard conditions. □ *= cyclohexene,* ◆ *= cyclohexene + benzaldehyde (0.136 mol · dm^{-3},* ◊ *= cyclohexene + phenylacetaldehyde (0.136 mol · dm^{-3}).* ■ *= cyclohexene (0.3 mol · dm^{-3}) + styrene (0.3 mol · dm^{-3}).*

increase in the epoxidation rate of the latter compound. Moreover, phenylacetaldehyde induces the same change in kinetics as styrene with respect to the reaction order in catalyst (Figure 9). In the presence of phenylacetaldehyde, the order in Mn(TP**P**)X remains one over the range $0 < [Mn(TPP)X] < 2.5 \cdot 10^{-3}$ mol · dm^{-3}. The rate-enhancing effect of phenylacetaldehyde decreases with increasing steric hindrance by the porphyrin catalyst [Mn(TP**P**)X > Mn(T$_{2,4,6}$triMeP**P**)X > Mn(T$_{2,6}$diClP**P**)X] (acceleration 4.1, 1.67, 1.15, respectively). The effects of some other aldehydes as well as ketones are summarized in Table V.

*Table V The effect of additives on the epoxidation rate of cyclohexene by Mn(TP**P**)X*[a].

Additive[b]	Relative rate
none	1[c]
2-naphthol	0.01
1-nitroso-2-maphthol	0.00
1-methylcyclohexene	0.80
cyclooctene	0.71
styrene	2.68
benzaldehyde	2.50
phenylacetaldehyde	4.10
3-phenylpropionaldehyde	2.60
propanal	1.60[d]
hexanal	1.90[d]
acetophenone	0.90
cyclohexanone	2.00
cyclopentanone	3.30

[a] Standard conditions. [b] [Additive] = 0.136 mol.dm^{-3}. [c] Epoxidation rate is $10.9 \cdot 10^{-5}$ mol · dm^{-3} · s^{-1}. [d] These compounds are rapidly oxidized to the corresponding carboxylic acids.

Aliphatic aldehydes have little effect mainly because they are rapidly oxidized to carboxylic acids. Aromatic aldehydes are only slowly converted into their corresponding carboxylic acids. Benzaldehyde, for example, is oxidized 7 times slower than cyclohexene under standard conditions: $k = 1.62 \cdot 10^{-5}$ and $10.91 \cdot 10^{-5}$ mol · dm^{-3} · s^{-1}, respectively[76].

Experiments performed with cyclohexene (0.626 mol · dm^{-3}), to which various amounts of benzaldehyde were added (0–0.450 mol · dm^{-3}), reveal that the enhancement in epoxidation rate is linear in aldehyde ($k_1 = 4.2 \pm 0.1$ s^{-1}). Substitution in the phenyl ring of benzaldehyde (4-NO$_2$, 4-F, 4-Me, and 4-MeO) has virtually no influence on the rate of epoxidation[41]. As was shown previously, little epoxidation takes place at pH 13.5 in the absence of a phase-transfer catalyst. Addition of aldehyde in this case did not induce a higher reaction rate, indicating that the aldehyde does not act as a phase-transfer catalyst for the hypochlorite anion. In the presence of MeOH (MeOH/CH_2Cl_2, 0.2 v/v *(vide supra)*, addition of phenylacetaldehyde still leads to acceleration of the epoxidation reaction. Without 4-methylpyridine, no rate-enhancing effect of aldehydes or ketones is observed, one again indicating the absolute necessity of pyridine as an axial ligand. Carbonyl compounds enhance the epoxidation reaction by rapidly trapping the oxo species thus preventing it *(i)* reverting to (**P**)MnOCl and *(ii)* reacting with [(**P**)Mn^{III}]$^+$ (Ref. 77).

Low-temperature experiments in which phenylacetaldehyde or cyclopentanone is added to a (**P**)MnOCl solution give profiles similar to those obtained with DPPH, including the burst. We propose that the carbonyl compound is converted into a dioxirane $\left(R_2C\langle^{O}_{O}\right)$ or carbonyl oxide ($R_2C{=}O^+ - -O^-$). Both species are powerful epoxidizing agents[78]. Experiments at low temperature in which ^{18}O-labeled cyclopentanone and cyclohexene were added simultaneously in a 25:1 ratio to (**P**)MnOCl showed no ^{18}O-incorporated epoxide. This implies that a carbonyl oxide had been formed, since in the case of dioxiranes 50% of the label would have been incorporated. The decrease in *cis/trans* epoxide ratio when *cis*-stilbene is used as a substrate also argues in favour of a carbonyl oxide species, since dioxiranes are known to epoxidize stereospecifically, in contrast to carbonyl oxides. The observed first order in catalyst for Mn(TP**P**)X in the presence of carbonyl compounds shows that these compounds suppress the dimerization reaction of [(**P**)MnO]$^+$ with [(**P**)Mn]$^+$ by trapping the former species. Sterically hindered catalysts are less susceptible to a bimolecular destruction reaction which is manifested by the modest carbonyl compound effects for these compounds.

d. Stereochemistry of the epoxidation reaction. The stereochemistry of the epoxidation reaction was probed by the use of *cis*-stilbene as the substrate. This compound gives two possible products: *cis*- and *trans*-stilbene oxide, of which the former is thermodynamically less favourable. Formation of *trans*-stilbene oxide requires rotation around the central C–C bond. The results of our experiments are given in Table VI.

cis-Stilbene is not isomerized to *trans*-stilbene under our reaction conditions. In the absence of any additive, *cis/trans* ratios of ≈ 1.6 and ≈ 19, are observed for Mn(TP**P**)X and the sterically hindered Mn(T$_{2,4,6}$triMeP**P**)X, respectively. The epoxidation mechanisms for Mn(TP**P**)X and Mn(T$_{2,4,6}$triMeP**P**)X are the same as judged from the ρ^+ values obtained by the experiments with substituted styrenes (see *Step 3b*). The isomerization shows that the epoxidation reaction is not concerted and that Van der Waals' interaction between catalyst and substrate may affect rotation in the intermediate[68]. Addition of pyridine (free or covalently bound) to Mn(TP**P**)X increases the *cis/trans* ratio up to 11.5 (see also Refs. 26 and 27). The results for compounds **P4**, **P8**, and **P11** show (see Table VI) that a decreasing spacer length gives a higher *cis/trans* ratio; the pyridine must, therefore, coordinate to the metal to exercise its influence. Addition of free pyridine to the catalysts containing covalently bound pyridine further increases the *cis/trans* ratio, indicating that the metal is not

Table VI The effect of additives on the stereoselectivity of the epoxidation of cis*-stilbene catalysed by various manganese porphyrins*[a].

Catalyst	4-Methyl-pyridine[b]	Methanol[c]	Phenyl-acetaldehyde[d]	*Cis/trans* ratio %/%
Mn(TPP)X	–	–	–	61/39
	+	–	–	92/8
	+	+	–	90/10
	–	+	–	69/31
	–	–	+	47/53
	+	–	+	79/21
Mn($T_{2,4,6}$triMePP)X	–	–	–	95/5
	–	–	+	85/15
P4	–	–	–	90/10
	+	–	–	95/5
	–	–	+	85/15
	+	–	+	90/10
P8	–	–	–	85/15
	+	–	–	89/11
	+	+	–	91/9
	–	+	–	80/29
	–	–	+	61/39
	+	–	+	86/14
P11	–	–	–	70/30
	+	–	–	90/10
	–	–	+	58/42
	+	–	+	85/15

[a] Standard conditions. [b] [4-Methylpyridine] = 1.3 mol · dm^{-3}. [c] $MeOH/CH_2Cl_2$ = 0.2 v/v. [d] [Phenylacetaldehyde] = 0.136 mol · dm^{-3}.

effectively tied up with the covalently bound pyridine molecule.

Two effects of pyridine on the *cis/trans* ratio can be visualized.

(i) An electronic effect. For the related Mn($T_{2,4,6}$triMePP)X/3-CPBA/*cis*-β-methylstyrene system, it was shown that the active [(**P**)MnO]$^+$ complex decays to the less reactive (**P**)Mn^{IV}=O species, which epoxidises less stereoselectively[17]. Pyridine could retard this process by stabilizing the high-valent [(**P**)MnO]$^+$ via electron donation.

(ii) A steric effect. Previously, we proposed that pyridine pulls the Mn centre into the plane of the porphyrin ligand, as shown schematically in Figure 10[68].

In intermediate **5a**, the steric barrier to rotation around the substrate C–C bond has increased as compared to **5b**. Consequently, stereoselectivity will be higher for **5a** than for **5b**.

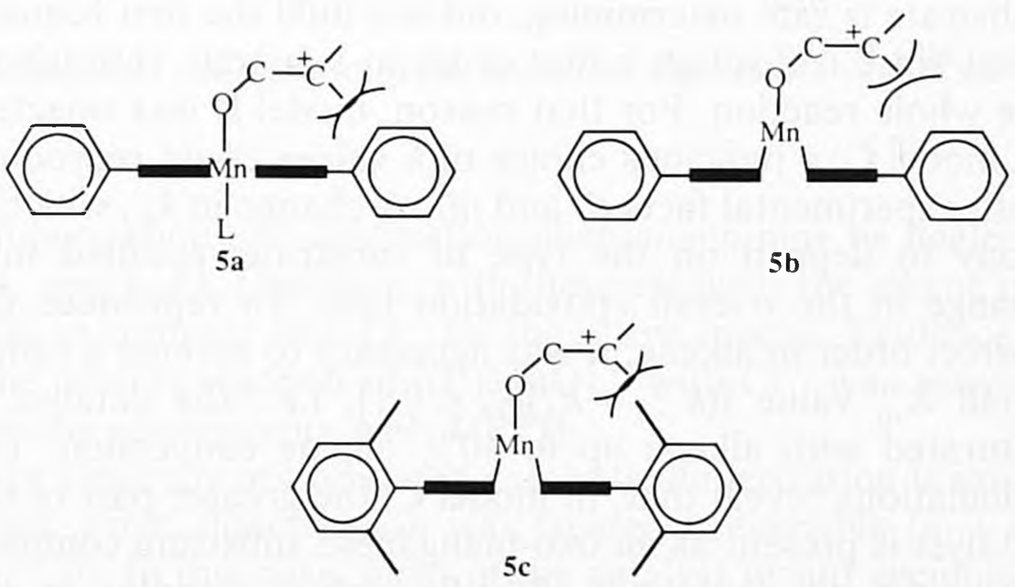

Fig. 10. The effect of pyridine (L) on the stereoselectivity of the epoxidation reaction. **5a**: *sterically not hindered porphyrin with pyridine;* **5b**: *sterically not hindered porphyrin without pyridine;* **5c**: *sterically hindered porphyrin.*

A similar effect is observed for porphyrins containing *ortho* substituents on their phenyl rings, **5c**.

Methanol has no effect on the *cis/trans* ratio. In the absence of pyridine, the addition of phenylacetaldehyde to Mn(TPP)X or Mn($T_{2,4,6}$triMePP)X markedly lowers the *cis/trans* ratio. Similar but less pronounced effects are observed in the presence of pyridine. Phenylacetaldehyde rapidly traps the [(**P**)MnO]$^+$ species *(vide supra)* to form a carbonyl oxide, which in turn acts as an epoxidizing agent[41]. Carbonyl oxides are known to epoxidise in a non-stereospecific way[78].

In the absence of 4-methylpyridine, no change in the *cis/trans* ratio is observed on lowering the pH [*cis/trans* ratio at pH 13.5 60/40, *cis/trans* ratio at pH 10.0 62/38][79]. Therefore, a change in mechanism as well as faster decomposition of the oxo-species-substrate complex upon lowering the pH may be excluded.

Step 4. [(**P**)MnO]$^+$ + [(**P**)Mn^{III}]$^+$ → [(**P**)Mn^{IV}–O–M^{IV}(**P**)]$^{2+}$ *or destructed porphyrin*

Manganese(III) tetraphenylporphyrin and derivatives thereof appear to be the only type of catalyst that displays a reasonable activity coupled to a high stability in the hypochlorite-based cytochrome-P-450 model. In general, the stability of these catalysts is high in the presence of reactive substrates, *e.g.*, cyclopentene, cyclohexene, cyclooctene, *cis*-stilbene, styrene, or norbornene. In the presence of less reactive substrates, *e.g.*, propene or 1-octene or in the absence of substrate, decomposition of the catalyst occurs. The decomposition is highly dependent on the type of catalyst used.

Catalyst destruction under standard reaction conditions, but in the absence of substrate, was studied by monitoring the decay of the Soret band of various porphyrins at low temperature. In the range down to 40% of the original amount of porphyrin, this decay could be fitted to a second-

order rate equation, indicating a bimolecular destruction process. A similar second-order process was found in the related cytochrome P-450 model, Fe(**P**)X/PhIO[4].

The catalyst destruction is most likely to proceed via electrophilic attack on the electron-rich *meso* positions of the porphyrin ring. The stability of the catalyst appears to be governed by steric and electronic factors. In general, large substituents (CH_3, OCH_3, Cl) at the 2- and 6-positions of the phenyl rings shield the reactive *meso* positions and thus adequately prevent attack at these sites.

Substitution at the 4-position of the phenyl rings shows that electronic factors also play a role. We found that electron-withdrawing substituents increase catalyst stability, whereas electron-donating substituents decrease it relative to TP**P**. This offers an explanation for the observation that single substitution at the 2-position by Cl and F is effective against catalyst destruction, whereas single substitution by CH_3 and OCH_3 is not. The role of fluorine substituents is puzzling. Substitution at the 2-position by F yields a very stable catalyst; this effect must be of electronic origin, given the small size of fluorine. However, the catalyst with four pentafluorophenyl groups is very unstable. Apparently, the presence of 20 fluorine substituents successfully activates the porphyrin ring for destructive nucleophilic attack. A similar effect might be expected for the pentachloro compound. In that case, however, the attack is prevented because of steric hindrance by the chlorine atoms.

It is tempting to suggest that the destruction is initiated by a reaction of $[(\mathbf{P})MnO]^+$ with $[(\mathbf{P})Mn^{III}]^+$ to form $[(\mathbf{P})Mn^{IV}-O-Mn^{IV}(\mathbf{P})]^{2+}$ μ-oxo dimer[5,6], after which oxidation of the reactive *meso* carbon atoms occurs, followed by opening of the porphyrin ring. *Ortho* substituents would prevent such dimerization and shield the *meso* positions. Experiments with PhIO and Mn(TP**P**)X have shown that μ-oxo dimers are formed in quantitative yield after short reaction times in the absence of substrate[5,6]. Longer reaction times gave bimolecular destruction of the porphyrin. Our view is further supported by the observation that treatment of the water-soluble Mn(T_4MePy**P**)Cl (in which $_4$MePy stands for 4-methyl-1-pyridinio), with hypochlorite results in the formation of a μ-oxo dimer[48]. The dimer decayed over a period of hours to Mn^{III}(**P**)X, a process in which 6–10% of the porphyrin ligand is destroyed. The isolation of maleimide, in that case, as a reaction product is in line with an initial attack on the *meso* positions.

Kinetic scheme

The overall epoxidation reaction in the Mn(**P**)X/hypochlorite system can be easily defined. The kinetics of the catalytic cycle, however, are a subject of discussion and disagreement. The case is complicated by the fact that each author uses his own reaction conditions, *e.g.*, as to type of porphyrin catalyst, axial ligand, substrate, pH of the aqueous phase, solvent, and concentration of the various components. In the preceding sections, it was shown that these factors exert a profound influence on the catalytic cycle. Since the catalytic cycle is rather complicated, we used a computer to simulate the various reaction conditions. The calculations are based on the reactions given in Scheme 3. In these calculations, the equilibria between the axial ligand (4-methylpyridine) and $[(\mathbf{P})Mn^{III}]^+$ have been neglected; we have assumed that all $[(\mathbf{P})Mn^{III}]^+$ exists as a mono-4-methylpyridine-ligated species throughout the complete catalytic cycle.

These simulations enabled us to evaluate and to substantiate the effect of substrate, added alcohols and carbonyl compounds, and catalyst structure. The curves calculated for epoxide formation and alkene conversion had to reproduce the following experimental facts:

(i) The reaction order in alkene is zero up to 40% alkene conversion and changes gradually to one with increasing alkene conversion;

(ii) Different alkenes are epoxidized at different rates.

We did not attempt to quantitative fit the calculated curves to the experimental data because of the large number of variables. Our calculations merely served to trace a trend. Three models were employed:

- formation of the oxo species is the rate-determining step (model **A**);
- formation of the oxo-**S** complex is the rate-determining step (model **B**);
- break-down of the oxo-**S** complex is the rate-determining step (model **C**).

Model **B**, in which the reaction of the $[(\mathbf{P})MnO]^+$ with the substrate is rate determining, did not fulfil the first requirement since it displays a first order in substrate throughout the whole reaction. For that reason, model **B** was rejected. In model **C**, a judicious choice of k values could reproduce both experimental facts *(i)* and *(ii)*. A change in k_4, which is likely to depend on the type of substrate, resulted in a change in the overall epoxidation rate. To reproduce the correct order in alkene, it was necessary to assume a rather small K_m value $[(k_{-3} + k_4)/k_3 < 0.1]$, *i.e.*, the catalyst is saturated with alkene up to 40% alkene conversion. The calculations reveal that, in model **C**, the greater part of the catalyst is present as an oxo-manganese substrate complex. However, we could not identify such a complex in the reaction mixture.

Model **A**, in which the formation of the active species is rate-determining, also reproduces the experimental results. Different rates are obtained for different alkenes by putting different k_3 values in the model. A high k_3 value means a reactive alkene, capable of competing favourably with Mn^{III}(**P**)X and Cl^- for the $[(\mathbf{P})MnO]^+$ species. As the substrate concentration becomes lower with progressing reaction, $k_3 \cdot [\mathbf{S}]$ becomes smaller than $k_{-2} \cdot [Cl^-]$ and/or $k_5 \cdot [Mn(\mathbf{P})Cl]$ and $k_6 \cdot [Mn(\mathbf{P})OCl]$. This indicates that the reaction with substrate gradually becomes rate-determining, in line with the observed shift in order in alkene towards one.

For sterically hindered catalysts, experiments showed that

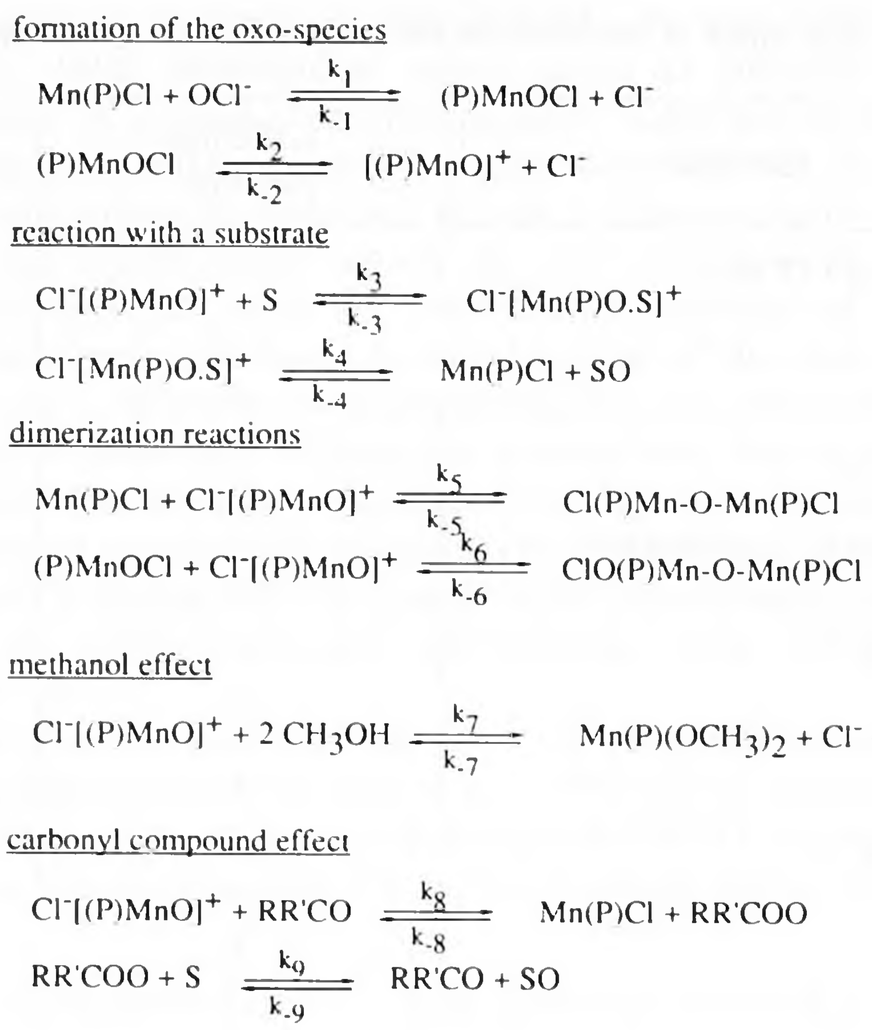

Scheme 3. Kinetic scheme used for computer simulations.

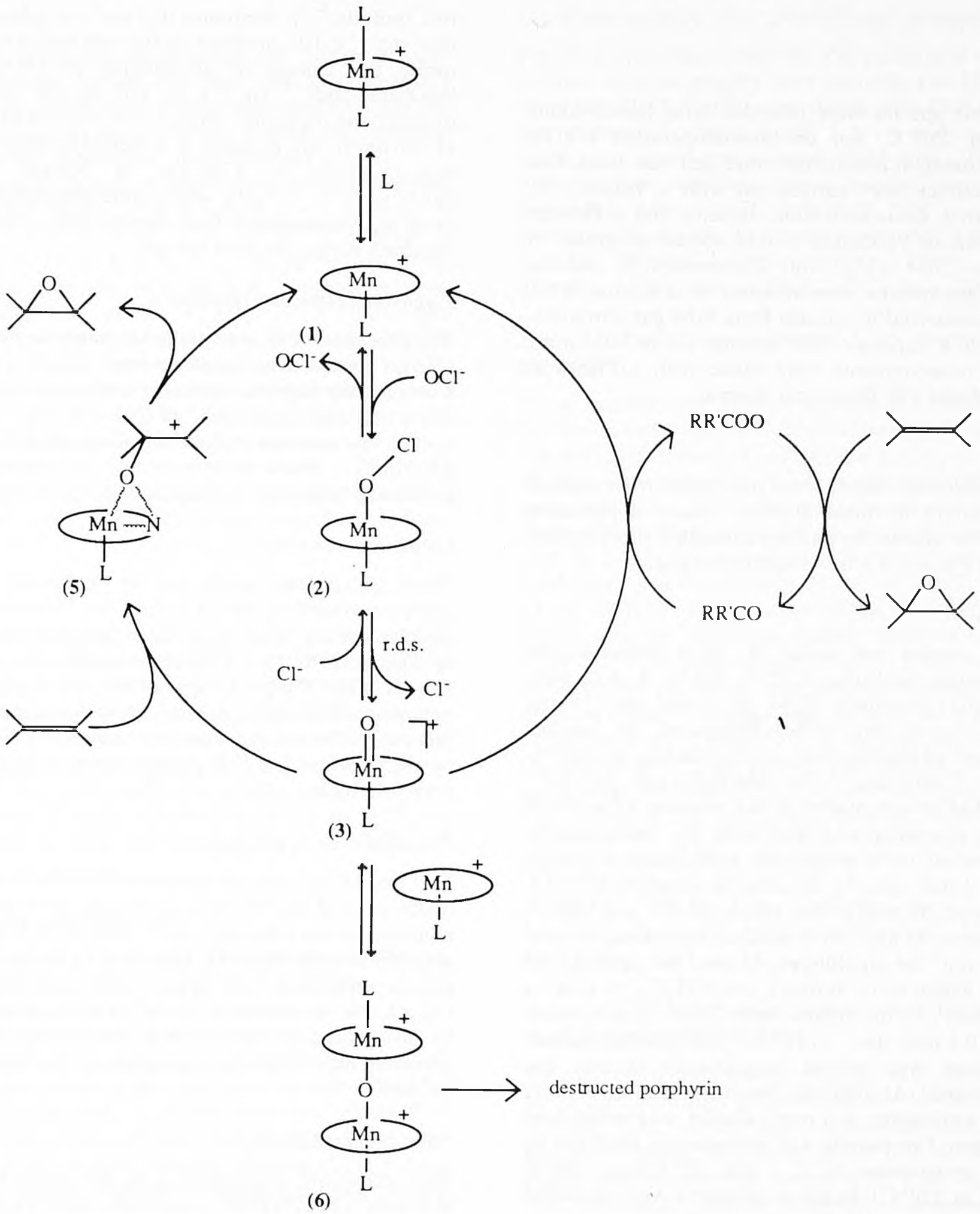

Scheme 4. Catalytic cycle based on the results described in this article.

dimerization and destruction phenomena may be neglected (k_5 and k_6 0). Therefore, with these catalysts the alkene only has to compete with Cl^- for the active species. Evidence for the reverse reaction of $[(\mathbf{P})MnO]^+$ with Cl^- was provided by the experiments with DPPH.

For sterically not hindered catalysts, dimerization is important. First, dimerization was treated irreversible (k_{-5} and k_{-6} 0). In this case, most of the catalyst would accumulate as μ-oxo dimer and the reaction would be first instead of zero order in substrate. Reversible dimer formation conditions under which $\approx 50\%$ of the catalyst exists as dimer, however, explained the experimental facts.

The effect of methanol is easily explained within model **A**. Due to an increased polarity of the organic phase, the formation of the active $[(\mathbf{P})MnO]^+$ is accelerated, *i.e.*, k_2 is larger. At higher concentrations, methanol competes with substrate for the active species to form an unreactive $Mn^{IV}(OCH_3)_2$ complex. The introduction of this possibility in the kinetic scheme produced the observed first order in substrate and the decrease in epoxidation rate upon addition of more than the optimum amount of methanol. The hydrophobic pocket of $Mn(T_{2,4,6}triMeP(\mathbf{P}))X$ reduces the effect of methanol; k_2 is less affected, predicting an almost zero-order-substrate dependence. Indeed, this behaviour is observed experimentally.

The effect of a lower pH of the aqueous phase, *i.e.*, a higher amount of HOCl present, is explained similar to that of methanol (k_2 becomes larger); in this case, however, no deactivation of the catalyst takes place.

To explain the effect of aldehydes and ketones, an additional step must be introduced in the reaction scheme. In this step, the carbonyl compound rapidly reacts with $[(\mathbf{P})MnO]^+$ (a large k_8) to produce a carbonyl oxide which, in turn, rapidly epoxidizes the alkene. In agreement with experiments, calculations predict a zero order in substrate and, for sterically hindered catalysts, a lower carbonyl effect than for those sterically not hindered, since one of the main modes of action of a carbonyl compound is to suppress dimerization effectively.

In summary, these simulations show that all kinetic observations are best explained by model **A**. The results of the present investigation are summarized in Scheme 4[80].

Experimental

Instrumentation

Ultraviolet and visible spectra were recorded on a Perkin-Elmer 555 spectrometer at 25.0°C. For the low-temperature UV/Vis measurements, a home-built low-temperature cell was used. Gas chromatographic analyses were carried out with a Varian 3700 Model equipped with a flame-ionization detector and a Hewlett Packard 3390 A model or Shimadzu C–R3A model integrator by using a Carbowax 20M (5%) on Chromosorb W column (2.50 m × 2 mm). Mass spectra were obtained on a Kratos MS80 mass spectrometer connected to a Carlo Erba 4160 gas chromatograph equipped with a capillary BP6 column (25 m × 0.1 mm). Cyclic-voltammetry measurements were made with a Princeton Applied Research Model 170 Electronic System.

Materials

Materials, unless otherwise noted, were purchased from Aldrich and purified by standard methods. Possible traces of peroxides were removed from the alkenes by passage through a short column of alumina (neutral, $l \times w = 5 \times 0.5$ cm) prior to use.

Epoxidation reactions

Epoxidations were carried out under N_2 in a Schlenk tube (5 × 0.8 cm), temperature-controlled at 25.0 ± 0.2°C. A stock solution of manganese(III) porphyrin ($3.94 \cdot 10^{-3}$ mol · dm^{-3}) and TEBACl ($7.88 \cdot 10^{-3}$ mol · dm^{-3}) was prepared in purified CH_2Cl_2, and 400 mm^3 of this solution (corresponding to concentrations of $2.5 \cdot 10^{-3}$ mol · dm^{-3} for Mn(**P**)X and $5.0 \cdot 10^{-3}$ mol · dm^{-3} for TEBACl) was placed in the reaction tube which had been previously evacuated and filled with N_2. Subsequently, the following compounds were added: the axial ligand 4-methylpyridine (80 mm^3, 1.3 mol · dm^{-3}), the internal standard for GLC (toluene or mesitylene, 10 mm^3), the alkene (0.626 mol · dm^{-3}, 40 mm^3 for cyclohexene, 47 mm^3 for 1-methylcyclohexene, 51 mm^3 for cyclooctene, 70 mm^3 for *cis*-stilbene, 45 mm^3 for styrene), an additive (methanol, aldehyde or ketone), and CH_2Cl_2 to make a total volume of 650 mm^3. To the organic layer, 2 cm^3 of an aqueous solution of NaOCl (0.4 mol · dm^{-3}, pH 13.5) was carefully added. The reaction mixture was stirred magnetically (stirrer bar 0.5 × 0.7 cm at 1100 rpm). At intervals, the stirrer and timer were stopped and, after separation, a 1 mm^3 aliquot was withdrawn from the organic layer. The sample was immediately analyzed by GLC (temperature programme 80°C 1 min, 25°C/min, 190°C 1 min or isothermal at 220°C). Reaction products were identified by GC/MS by comparison with authentic samples.

All reactions were carried out at pH 13.5 of the aqueous phase to avoid side reactions involving halohydrin[81] or ClO• routes[82], which become operative at pH less than 10. Control experiments at pH 13.5 showed almost no conversion of cyclohexene in the absence of catalyst. In the presence of catalyst, the main product of the oxidation of cyclohexene at pH 13.5 is the epoxide. Only trace amounts (< 1%) of the allylic oxidation products 2-cyclohexenol and 2-cyclohexenone were detected. Although the amounts of by-products are by and large minor, control experiments established that they are formed during the course of epoxidation and not in a subsequent rearrangement of the epoxide. On the other hand, none of these products could be converted into the epoxide. This proves that they do not act as intermediates in the epoxidation reaction.

Standard conditions imply the use of Mn(TP**P**)X (catalyst), cyclohexene (substrate) and 4-methylpyridine (axial ligand) in concentrations as listed above.

UV/Vis experiments

All low-temperature experiments were carried out under N_2. A 1-cm quartz cell filled with a solution of Mn($T_{2,4,6}$triMeP**P**)Cl or Mn($T_{2,6}$diClP**P**)Cl in CH_2Cl_2 (3 cm^3, $2.25 \cdot 10^{-5}$ mol · dm^{-3}) was placed in the low-temperature device and allowed to cool to −50°C. Thereafter, TEBAOCl dissolved in CH_2Cl_2, was added by syringe until the Mn(III) peak at 478 nm had decreased to ≈5% of its original height (about 0.1 cm^3 were required). After further equilibrating for 15 min, 0.1 cm^3 of CH_2Cl_2 containing DPPH ($7 \cdot 10^{-3}$ mol · dm^{-3}) was added and, optionally, 4-methylpyridine (0.2 mol · dm^{-3}), methanol (0.5 cm^3) or phenylacetaldehyde (0.1 mol · dm^{-3}). The progress of the reaction was followed by monitoring the change in absorbance at 478 nm [[(**P**)Mn(III)]$^+$, $\log(\varepsilon/\text{dm}^3 \cdot \text{mol}^{-1} \cdot \text{cm}^{-1}) = 5.08$ in the absence of 4-methylpyridine and $\log(\varepsilon/\text{dm}^3 \cdot \text{mol}^{-1} \cdot \text{cm}^{-1}) = 4.89$ in its presence] and at 520 nm in the absence of 4-methylpyridine [DPP•, $\log(\varepsilon/\text{dm}^3 \cdot \text{mol}^{-1} \cdot \text{cm}^{-1}) = 4.38$] or at 530 nm DPP•, $\log(\varepsilon/\text{dm}^3 \cdot \text{mol}^{-1} \cdot \text{cm}^{-1}) = 4.39$] when 4-methylpyridine is present. Initial rates were determined from pseudo-zero-order plots of the data obtained during the first minute.

Porphyrin destruction reactions

The procedure was essentially the same as for the epoxidation of alkenes except that substrate was absent. At regular intervals, 8 mm^3 of the organic layer was withdrawn and added by syringe into a cell containing 2 cm^3 of 0.01 mol · dm^{-3} PPh_3 in CH_2Cl_2 to quench the reaction and to transform all porphyrinic material to [(**P**)Mn^{III}]$^+$. Blank experiments, in the absence of oxidant, were performed to ensure the reproducibility of the method.

Labeling experiments

These experiments could not be performed under normal two-phase conditions at pH 13.5 since the ^{18}O-labeled cyclopentanone rapidly lost its label in a base-catalysed reaction. Therefore, a set-up similar to the UV/Vis experiments was employed. After generation of the (**P**)MnOCl species at −50°C, 10 mm^3 of ^{18}O-labeled cyclopentanone and 100 mm^3 of cyclohexene were added simultaneously. The mixture was concentrated to 100 mm^3 and analysed by GC/MS for the ^{18}O content of both cyclohexene oxide and cyclopentanone.

^{18}O-labeled cyclopentanone

To 1 cm^3 (0.011 mol) of cyclopentanone in a small test tube, 1 cm^3 (0.056 mol) of $H_2{}^{18}O$ (50% enriched), 20 drops of 1,4-dioxane (to homogenize the solution), and 1 drop of H_2SO_4 were added. Upon addition of solid $NaHCO_3$ after 24 h to neutralize the solution, two phases separated. The upper layer was diluted with 1 cm^3 of CH_2Cl_2 and washed with 10 cm^3 of H_2O. After removal of CH_2Cl_2 by distillation, 0.9 cm^3 of 50% ^{18}O-enriched cyclopentanone was obtained, n_D^{20} 1.4363. Incorporation of the label was confirmed by GC/MS.

^{18}O-labeled TEBAOCl

This compound was prepared by dissolving 100 mg of TEBAOCl in 0.3 cm^3 of $H_2{}^{18}O$ (50% enriched, Alpha) followed by removal of the solvent. The procedure was repeated twice.

Cyclic voltammetry

Since the chloride redox couple interferes heavily with the voltammograms of Mn(**P**)X, it is essential to work under chloride-free conditions. For that reason, the Mn complexes were measured as perchlorate derivatives. Methylene chloride, which contains free HCl, was washed with a 5% $NaHCO_3$ aqueous solution and then water, dried over $CaCl_2$, and distilled from P_2O_5.

In a typical procedure, the voltammetry cell, temperature-controlled at 25°C, was fit with a freshly polished (Al_2O_3) platinum working electrode (wire, 1 × 0.1 cm), and platinum counter electrode (foil, 1 × 1 cm). The reference electrode consisted of a saturated sodium calomel electrode in water, and was separated from the voltammetry cell by salt bridges in the following way: The bridge adjacent to the reference electrode contained 0.1 mol · dm^{-3} NaCl aqueous solution and that adjacent to the voltammetry cell contained the same medium as used for the sample. The cell was then charged with 50 cm^3 of a $50 \cdot 10^{-3}$ mol · dm^{-3} Mn(**P**)X solution in purified CH_2Cl_2 with 0.1 mol · dm^{-3} TBAP as supporting electrolyte. All solvent/supporting electrolyte solutions were deaerated with solvent-saturated N_2 before solid porphyrin was added. A nitrogen stream was also passed over the solutions during the measurements. When the cyclic voltammogram had been recorded (sweep rate 100 mV/s, no iR compensation, filter 30 ms), some solid ferrocene was added such that the ferrocene concentration was $5 \cdot 10^{-4}$ mol · dm^{-3}. The potential and electrochemical reversibility of the ferrocene/ferrocenium ion redox couple was recorded and used as an internal standard[83] (E° = 0.400 V *versus* NHE[84]).

Kinetic simulations

Using Scheme 3, differential equations giving the change in concentration of each species present per time unit (d[species]/dt) were derived. These equations were solved numerically to give the concentration of each species as a function of time. (A complete listing of the programme is available upon request.)
Numerical input: Model **B** (formation of the oxo-substrate complex is rate-determining) $k_1 = 10$, $k_{-1} = 1$, $k_2 = 1$, $k_{-2} = 1$, $k_3 = 10^{-2}$, $k_{-3} = 0$, $k_4 = 1$, $k_{-4} = 0$, $k_5 = 10^{-2}$, $k_{-5} = 10^{-2}$, $k_6 = 10^{-2}$, $k_{-6} = 10^{-2}$, $k_7 = 0$, $k_{-7} = 0$, $k_8 = 0$, $k_{-8} = 0$, $k_9 = 0$, $k_{-9} = 0$. Model **C** (decomposition of the oxo-substrate complex is rate-determining), see model **B**, except $k_3 = 1$, $k_{-3} = 10^{-1}$, and $k_4 = 5 \cdot 10^{-2}$ highly reactive substrate; $k_4 = 10^{-2}$ substrate of normal reactivity; $k_4 = 5 \cdot 10^{-3}$, substrate of low activity.
Model **A** (formation of the oxo species is rate-determining), see model **B**, except $k_2 = 10^{-2}$, $k_{-2} = 2 \cdot 10^{-2}$ and $k_3 = 10$ highly reactive substrate; $k_3 = 1$ substrate of normal reactivity; $k_3 = 10^{-1}$, substrate of low reactivity.
Initial concentrations in all models: [Mn(**P**)X] = 10^{-2}, OCl^-] = 0.3, [alkene] = 0.1, [Cl^-] = 0.3, [methanol] = 0.1, [carbonyl compound] = 10^{-2}.

Porphyrins

The porphyrin ligands were prepared according to published procedures: T_2ClPP[85], T_4ClPP[85], T_2FPP[85], T_4FPP[85], TPP[86], T_4MePP[85], T_4MeOPP[85], $T_4(NMe_2)PP$[85], T_4NO_2PP[87]. $T_{2,4,6}$-triMePP, $T_{2,6}$diClPP, TpentaFPP, and $T_{2,4,6}$triMeOPP were prepared according to Ref. 88 with 2.5 mol·dm^{-3} (instead of 0.5 mol·dm^{-3}) BF_3·etherate complex as a catalyst. For the synthesis of $T_{2,4,6}$triMePP and $T_{2,4,6}$triMeOPP, the addition of 0.75% (v/v) MeOH or EtOH to the CH_2Cl_2 solvent was found to be highly beneficial with respect to yield and reaction rate. ^{1}H NMR and UV/Vis spectra were as reported.

3-(3-Bromopropyl)pyridine hydrobromide

3-(3-Pyridyl)propanol (5.49 g, 40 mmol) was refluxed with 40 cm^3 of an aqueous HBr solution (48%) under N_2 for 5 h. During this period, the originally light-brown solution darkened. After completion of the reaction, the water was removed on a rotavap/oil-pump combination. A viscous brown oil was obtained, which crystallized upon standing. Recrystallization from 25 cm^3 of acetone gave off-white platelets. A second crop was obtained on concentrating the filtrate to 10 cm^3 and allowing it to stand overnight at −40 °C. IR (KBr) showed the total absence of the starting alcohol and a C–Br band at 680 cm^{-1}. Yield 4.5 g (40%); m.p. 107.3 °C.

3-[[2-(2-Chloroethoxy)ethoxy]methyl]pyridine

To a stirred solution of 3-(hydroxymethyl)pyridine (2.07 g, 20 mmol) in 25 cm^3 of DMF, 1–chloro-2-(2-tosylethoxy)ethane (5.3 g, 20 mmol) and powdered KOH (2 g, 35.7 mmol) were added under N_2. After 16 h, the KOH was removed by filtration and 150 cm^3 of CH_2Cl_2 were added. The resulting solution was washed with water (10 × 50 cm^3) and then dried ($MgSO_4$). After evaporation of the solvent, the product was obtained as a yellow oil. Yield 2.37 g (55%). ^{1}H NMR ($CDCl_3$) δ: 8.4 (br m, 2H, PyH), 7.8–8.0 (br m, 2H, PyH), 4.5 (s, 2H, $-OCH_2Py$), 3.6 [s, 8H, $-(OCH_2CH_2)_2Cl$]; ^{1}H NMR showed the presence of ≈10% of DMF.

3-[[2-[2-(2-Chloroethoxy)ethoxy]ethoxy]methyl]pyridine

This compound was prepared in a similar way as described for 3-[[2-(2-chloroethoxy)ethoxy]methyl]pyridine except that 1-chloro-2-(2-tosylethoxy)ethane was substituted by 1-chloro-2-[2-(2-tosylethoxy)ethoxy]ethane (6.18 g, 20 mmol). The product was obtained as a yellow oil. Yield 2.70 g (52%). ^{1}H NMR ($CDCl_3$) δ: 8.4 (br m, 2H, PyH), 7.8–8.0 (br m, 2H, PyH), 4.5 (s, 2H, $-OCH_2Py$), 3.2–3.6 [s, 12H, $-(OCH_2CH_2)_3Cl$]; ^{1}H NMR showed the presence of ≈5% of DMF.
The following porphyrins, containing a covalently attached pyridine molecule, are denoted by the short-hand notation **P*n***, with ***n*** being the number of spacer atoms. Structure and adopted lettering for ^{1}H NMR are presented in Figure 1.

*5-(2-Hydroxyphenyl)-10,15,20-tris(4-methylphenyl)porphyrin**

Prepared according to Ref. 89. The compound was purified by dry-column chromatography over alumina (act III, $l \times w$ 40 × 4 cm). First, the $H_2(T_4MePP)$ was eluted with $CHCl_3$, then the eluent was changed to $CHCl_3$/EtOH 5:1 v/v and the product was collected as a broad purple band. Yield 10%. ^{1}H NMR ($CDCl_3$) δ: 8.82 (s + three satellites due to unequal β-pyrrole protons, 8H, β-pyrrole), 8.04 (d, 6H, 2,6-tolyl), 7.94 (d, 1H, 6-(2-hydroxyphenyl)), 7.67 (t, 1H, 4-(2-hydroxyphenyl)), 7.50 (d, 6H, 3,5-tolyl), 7.31 (d, 1H, 3-(2-hydroxyphenyl)), 7.28 (t, 1H, 5-(2-hydroxyphenyl)), 2.65 (s, 9H, $-CH_3$), −2.79 (br s, 2H, NH).

5-[2-[3-(3-Pyridyl)propoxy]phenyl]-10,15,20-tris(4-methylphenyl)porphyrin (**P4**)

To a magnetically stirred solution of 250 mg (0.37 mmol) of 5-(2-hydroxyphenyl)-10,15,20-tris(4-methylphenyl)porphyrin and 750 mg (5.43 mmol) of anhydrous K_2CO_3 in 7.5 cm^3 of DMF, 115 mg (0.41 mmol) of 3-(3-bromopropyl)pyridine was added at once. After 4 h at 40 °C, the reaction was complete as indicated by TLC (silica; eluent: ethyl acetate, starting compound R_f 0.95; product R_f 0.65). The solvent was removed under vacuum and the solid mass was dissolved in 25 cm^3 of $CHCl_3$ and extracted with 25 cm^3 of H_2O. The aqueous phase was washed with 10 cm^3 of $CHCl_3$ and the combined organic fractions were extracted with 25 cm^3 of H_2O. After drying ($MgSO_4$), the organic solution was concentrated to 10 cm^3 and chromatographed over silica under pressure (eluent: ethyl acetate, column: 20 × 2 cm). After a small amount of starting porphyrin (10 mg), the desired product came off the column as a broad purple band. Yield 150 mg (50%, based on porphyrin). ^{1}H NMR ($CDCl_3$) (lettering corresponds to Figure 1) δ: −2.70 (br s, 2H, a), 1.25 (t, 2H, k), 1.54 (m, 2H, l), 2.69 (s, 9H, e), 3.85 (t, 2H, j), 5.90 (d, 1H, n), 6.22 (m, 1H, m), 7.2–8.2 (m, 8H, c,d,f,g,h,i,o,p), 8.83 (m, 8H,b).

Mn(P4)Cl. UV/Vis λ/nm [log(ε/dm^3·mol^{-1}·cm^{-1})] (CH_2Cl_2): 342 (4.60), 384 (4.69), 410 (4.60), 476 (4.82), 520 (3.90), 576 (3.98), 616 (4.02).

5-[2-[2-(2-(3-Pyridyl)methoxy]ethoxy]ethoxy]phenyl]-10,15,20-tris(4-methylphenyl)porphyrin (**P8**)

To solution of 5-(2-hydroxyphenyl)-10,15,20-tris(4-methylphenyl)-porphyrin (250 mg, 0.37 mmol) in 7.5 cm^3 of DMF, K_2CO_3 (750 mg, 5.43 mmol) and 3-[[2-(2-chloroethoxy)ethoxy]methyl]-pyridine (200 mg, containing about 10% DMF, 0.75 mmol) were added. The mixture was stirred at 70 °C for 24 h. After this period, TLC indicated almost complete conversion of the starting compound (silica, eluent: ethyl acetate; starting compound R_f 0.95, product $R_f \approx 0.6$). After removal of the solvent, the purple product was dissolved in 50 cm^3 of $CHCl_3$ and extracted with an equal volume of water. The aqueous layer was washed with 10 cm^3 of $CHCl_3$ and the combined $CHCl_3$ fractions were extracted with 50 cm^3 of H_2O. After drying ($MgSO_4$), the solvent was removed and the product dissolved in 10 cm^3 of ethyl ecetate. Chromatography under pressure (silica; eluent ethyl acetate; column 15 × 4 cm) yielded the product as a purple powder (285 mg, 90%, based on starting porphyrin). ^{1}H NMR ($CDCl_3$) (lettering corresponds to Figure 1) δ: −2.85 (br s, 2H, a), 1.72 (t, 2H, r), 2.04 (t, 2H, q), 2.61 (s, 9H, e), 2.76 (s, 2H, s), 2.94 (t, 2H, k), 3.94 (t, 2H, j), 6.38 (m, 1H, n), 6.56 (d, 1H, m), 7.23 + 7.31 (d + d, 2H, f,h), 7.46 (d, 6H, d), 7.71 (d + d, 2H, g,i), 7.97 (d, 6H, c), 8.03 (s, 1H, p), 8.72 − 8.79 (s, 8H, b), 8.12 (d, 1H, o).

Mn(P8)Cl. UV/Vis λ/nm [log(ε/dm^3·mol^{-1}·cm^{-1})] (CH_2Cl_2): 376 (4.79), 403 (4.74), 478 (5.09), 528 (3.89), 578 (4.07), 616 (4.14).

5-[2-[2-(2-(2-(3-Pyridylmethoxy)ethoxy)ethoxy)ethoxy]phenyl]-10,15,20-tris(4-methylphenyl)porphyrin (**P11**)

This compound was prepared similar to **P8** except that 3-[(2-[2-chloroethoxy]ethoxy)methyl]pyridine was substituted by 3-[(2-[2-(2-chloroethoxy)ethoxy]ethoxy)methyl]pyridine (240 mg,

---

* Porphyrin is indexed in *Chem. Abstr.* as 21*H*,23*H*-porphine.

containing about 10% DMF, 0.75 mmol). Yield (300 mg, 90%, based on starting porphyrin). ^{1}H NMR ($CDCl_3$) (lettering corresponds to Figure 1) δ: −2.85 (br s, 2H, a), 1.72 (t, 2H, r), 2.04 (t, 2H, q), 2.61 (s, 9H, e), 2.76 (s, 2H, s), 2.94 (t, 2H, k), 3.94 (t, 2H, j), 6.38 (m, 1H, n), 6.56 (d, 1H, m), 7.23 + 7.31 (d + d, 2H, f,h), 7.46 (d, 6H, d), 7.71 (d + d, 2H, g,i), 7.97 (d, 6H, c), 8.03 (s, 1H, p), 8.72 − 8.79 (s, 8H, b), 8.12 (d, 1H, o).

*Mn(**P11**)Cl.* UV/Vis λ/nm [log (ε/dm^3 · mol^{-1} · cm^{-1})] (CH_2Cl_2): 344 (4.57), 376 (4.72), 396 (4.69), 476 (5.13), 522 (3.83), 575 (4.09), 610 (4.05).

Acknowledgements

The authors owe their thanks to Miss *J. C. M. Bax*, Miss *C. B. Hansen*, Miss *P. M. F. C. Groot* and Mr. *M. J. P. van Gerwen* for experimental assistance, to Dr. *A. M. F. Hezemans* for writing the programme for the kinetic simulations, to Prof. *D. W. H. den Boer*, Dr. *J. H. van Lenthe*, and Miss *R. Zwaans* for their help with the quantum-chemical calculations, and to Mr. *G. H. Pellaerts* for the construction of the low-temperature UV/Vis cell. This research was supported by the Netherlands Foundation for Chemical Research (SON) with financial aid from the Netherlands Foundation for Scientific Research (NWO).

References

[1] *J. T. Groves* and *P. Viski*, J. Am. Chem. Soc. **111**, 8537 (1989) and references cited therein.
[2] *J. T. Groves*, *W. J. Kruper, Jr.* and *R. C. Haushalter*, J. Am. Chem. Soc. **102**, 6375 (1980).
[3] *C. L. Hill* and *B. C. Schardt*, J. Am. Chem. Soc. **102**, 6374 (1980).
[4] *M. J. Nappa* and *C. A. Tolman*, Inorg. Chem. **24**, 4711 (1985).
[5] *B. C. Schardt*, *F. J. Hollander* and *C. L. Hill*, J. Am. Chem. Soc. **104**, 3964 (1982).
[6] *J. A. Smegal* and *C. L. Hill*, J. Am. Chem. Soc. **105**, 3515 (1983).
[7] *B. R. Cook*, *T. J. Reinert* and *K. S. Suslick*, J. Am. Chem. Soc. **108**, 7286 (1986).
[8] *J. P. Collman*, *T. Kodadek*, *S. A. Raybuck*, *J. J. Brauman* and *L. M. Papazian*, J. Am. Chem. Soc. **107**, 4343 (1985).
[9] *T. G. Traylor*, *T. Nakano*, *A. R. Miksztal* and *B. E. Dunlap*, J. Am. Chem. Soc. **109**, 3625 (1987).
[10] *T. G. Traylor* and *A. T. Miksztal*, J. Am. Chem. Soc. **109**, 2770 (1987) and references cited therein.
[11] *T. G. Traylor* and *F. Xu*, J. Am. Chem. Soc. **110**, 1953 (1988).
[12] *P. N. Balasubramanian*, *A. Sinha* and *T. C. Bruice*, J. Am. Chem. Soc. **109**, 1456 (1987).
[13] *G. Legemaat*, Ph.D. thesis, Utrecht, 1990.
[14] *P. Battioni*, *J. P. Renaud*, *J. F. Bartoli*, *M. Reina-Artiles*, *M. Fort* and *D. Mansuy*, J. Am. Chem. Soc. **110**, 8462 (1988) and references cited therein.
[15] *P. L. Anelli*, *S. Banti*, *F. Montanari* and *S. Quici*, J. Chem. Soc., Chem. Commun. 779 (1989).
[16] *J. T. Groves* and *M. K. Stern*, J. Am. Chem. Soc. **110**, 8628 (1988) and references cited therein.
[17] *J. T. Groves* and *M. K. Stern*, J. Am. Chem. Soc. **109**, 3812 (1987).
[18] *J. T. Groves* and *Y. Watanabe*, J. Am. Chem. Soc. **108**, 507 (1986).
[19] *J. T. Groves* and *Y. Watanabe*, Inorg. Chem. **26**, 785 (1987).
[20] *W.-H. Wong*, *D. Ostovic* and *T. C. Bruice*, J. Am. Chem. Soc. **109**, 3428 (1987) and references cited therein.
[21] *C. M. Dicken*, *T. C. Woon* and *T. C. Bruice*, J. Am. Chem. Soc. **108**, 1636 (1986).
[22] *T. C. Woon*, *C. M. Dicken* and *T. C. Bruice*, J. Am. Chem. Soc. **108**, 7990 (1986).
[23] *I. Tabushi* and *N. Koga*, Tetrahedron Lett. **20**, 3681 (1979).
[24] *E. Guilmet* and *B. Meunier*, Tetrahedron Lett. **21**, 4449 (1980).
[25] *E. Guilmet* and *B. Meunier*, Tetrahedron Lett. **23**, 2449 (1982).
[26] *E. Guilmet* and *B. Meunier*, Nouv. J. Chim. **6**, 511 (1982).
[27] *B. Meunier*, *E. Guimet*, *M.-E. de Carvalho* and *R. Poilblanc*, J. Am. Chem. Soc. **106**, 6668 (1984).
[28] *J. P. Collman*, *T. Kodadek*, *S. A. Raybuck* and *B. Meunier*, Proc. Natl. Acad. Sci. U.S.A. **80**, 7039 (1983).
[29] *J. P. Collman*, *J. J. Brauman*, *B. Meunier*, *S. A. Raybuck* and *T. Kodadek*, Proc. Natl. Acad. Sci. U.S.A. **81**, 3245 (1984).
[30] *J. P. Collman*, *J. J. Brauman*, *B. Meunier*, *T. Hayashi* and *T. Kodadek*, J. Am. Chem. Soc. **107**, 2000 (1985).
[31] *J. P. Collman*, *T. Kodadek* and *J. I. Brauman*, J. Am. Chem. Soc. **108**, 2588 (1986).
[32] *A. W. van der Made*, *J. W. H. Smeets*, *R. J. M. Nolte* and *W. Drenth*, J. Chem. Soc., Chem. Commun. 1204 (1983).
[33] *J. A. S. J. Razenberg*, *R. J. M. Nolte* and *W. Drenth*, Tetrahedron Lett. **25**, 789 (1984).
[34] *J. A. S. J. Razenberg*, *A. W. van der Made*, *J. W. H. Smeets* and *R. J. M. Nolte*, J. Mol. Catal. **31**, 271 (1985).
[35] *B. Meunier*, *M.-E. de Carvalho* and *A. Robert*, J. Mol. Catal. **41**, 185 (1987) and references cited therein.
[36] *J. A. S. J. Razenberg*, *R. J. M. Nolte* and *W. Drenth*, J. Chem. Soc., Chem. Commun. 277 (1986).
[37] *R. J. M. Nolte*, *J. A. S. J. Razenberg* and *R. Schuurman*, J. Am. Chem. Soc. **108**, 2751 (1986).
[38] *O. Bortolini*, *M. Ricci*, *B. Meunier*, *P. Friant*, *I. Ascone* and *J. Goulon*, Nouv. J. Chim. **10**, 39 (1986).
[39] *F. Montanari*, *M. Penso*, *S. Quici* and *P. Vigano*, J. Org. Chem. **50**, 4888 (1985).
[40] *R. W. Lee*, *P. C. Nakagaki* and *T. C. Bruice*, Proc. Natl. Acad. Sci. U.S.A. **85**, 641 (1988).
[41] *A. W. van der Made*, *M. J. P. van Gerwen* and *R. J. M. Nolte*, J. Chem. Soc., Chem. Commun. 888 (1987).
[42] *O. Bortolini* and *B. Meunier*, J. Chem. Soc., Perkin Trans. II 1967 (1984).
[43] *K. S. Suslick* and *B. R. Cook*, J. Chem. Soc., Chem. Commun. 200 (1987).
[44] Since the distribution of OCl^- over the two phases cannot be determined accurately, it was assumed that $[OCl^-]_{org.} = [OCl^-]_{aq.}$. In practice, $[OCl^-]_{org.} \ll [OCl^-]_{aq.}$ because of *(i)* the limited solubility of OCl^- in (wet) CH_2Cl_2 and *(ii)* the limited amount of p.t.c. present in the organic phase. For these reasons, the calculated K_m value represents the upper limit, *i.e.*, the actual affinity of Mn(**P**)Cl for OCl^- is higher.
[45] *A. W. van der Made*, *P. M. F. C. Groot*, *W. Drenth* and *R. J. M. Nolte*, Recl. Trav. Chim. Pays-Bas **108**, 73 (1989).
[46] *N. Carnieri*, *A. Harriman* and *G. Porter*, J. Chem. Soc. Dalton Trans. 931 (1982).
[47] *N. Carnieri*, *A. Harriman*, *G. Porter* and *K. Kalyanasundaram*, J. Chem. Soc., Dalton Trans. 1231 (1982).
[48] *L. O. Spreer*, *A. Leone*, *A. C. Maliyackel*, *J. W. Otvos* and *M. Calvin*, Inorg. Chem. **27**, 2401 (1988).
[49] In a preliminary communication (*A. W. van der Made*, *W. Drenth* and *R. J. M. Nolte*, Recl. Trav. Chim. Pays-Bas **106**, 330 (1987)), this species was incorrectly identified as a manganese(V)-oxo species.
[50] See also ref. 38, although the species described therein is not explicitly identified as (**P**)MnOCl.
[51] See also *K. R. Rodgers* and *H. M. Goff*, J. Am. Chem. Soc. **110**, 7049 (1988).
[52] Abbreviated names of catalysts; TP**P** = 5,10,15,20-tetraphenylporphyrinato. The other catalysts have substituents on their phenyl rings: 2,4,6-triMe; 2,4,6-triPh; 2,4,6-triMeO; 2,6-diCl; 2-Cl; 2-F; 2-CH_3O; 4-CH_3O; 2-CH_3; 4-CH_3; penta-F.
[53] No hypochlorite transition metal complexes have been published. Apparently, the porphyrin ligand provides adequate electronic and steric stabilization of the MnOCl complex, in contrast to simple metal complexes where oxidation of the metal occurs. To distinguish the complex from an ionic OCl^- complex, the designation (P)MnOCl is used.
[54] Halogen oxidation is not without precedent in cytochrome P-450 chemistry. The active species generated by the action of PhIO on cytochrome P-450 was shown to oxidize PhI to PhIO:

$$Ph^{125}I + PhIO \underset{\longleftarrow}{\overset{\text{cytochrome P-450}}{\longrightarrow}} Ph^{125}IO + PhI$$

See *L. T. Burka*, *A. Thorsen* and *F. P. Guengerich*, J. Am. Chem. Soc. **102**, 7615 (1980).

[55] *B. C. Schardt, F. Hollander* and *C. L. Hill*, J. Chem. Soc., Chem. Commun. 765 (1981).

[56] *B. C. Schardt, F. Hollander* and *C. L. Hill*, J. Am. Chem. Soc. **104**, 3964 (1982).

[57] *L.-C. Yuan* and *T. C. Bruice*, J. Am. Chem. Soc. **108**, 1643 (1986).

[58] A GC/MS analysis shows the presence of hydroxylated, chlorinated, and ring-opened products derived from NAcPhIm.

[59] *M. J. Camenzind, R. J. Hollander* and *C. L. Hill*, Inorg. Chem. **21**, 4301 (1982).

[60] *F. Montanari* and *S. Quici*, La Chimica et L'industria (Ital.) **68**, 72 (1986).

[61] *S. Banfi, F. Montanari* and *S. Quici*, J. Org. Chem. **53**, 2863 (1988).

[62] *S. Banfi, F. Montanari* and *S. Quici*, Recl. Trav. Chim. Pays-Bas **109**, 117 (1990).

[63] *A. W. van der Made, J. M. C. Bax, W. Drenth* and *R. J. M. Nolte*, Recl. Trav. Chim. Pays-Bas **108**, 185 (1989).

[64] *D. W. H. den Boer, J. H. van Lenthe* and *A. W. van der Made*, Recl. Trav. Chim. Pays-Bas **107**, 256 (1988).

[65] *D. W. H. den Boer, A. W. van der Made, R. Zwaans* and *J. H. van Lenthe*, Recl. Trav. Chim. Pays-Bas **109**, 123 (1990).

[66] Identical values are reported in Ref. 42. For the PhIO/Fe(TP**P**)X system a ρ^+ of -0.93 is found (see Ref. 1g). Based on UV/Vis experiments, ρ^+ -1.90 reported for $Fe^{III}(T_{2,4,6}$triMe**PP**$)OH$/3-CPBA (see Ref. 18).

[67] *R. P. Hanzlik* and *G. O. Shearer*, J. Am. Chem. Soc. **97**, 5231 (1975).

[68] *A. W. van der Made* and *R. J. M. Nolte*, J. Mol. Catal. **26**, 333 (1984).

[69] *M. Schappacher* and *R. Weiss*, Inorg. Chem. **26**, 1189 (1987).

[70] The suggestion by *Goff* et al. (Ref. 51) that pyridine might suppress porphyrin-catalysed chlorination reactions is not supported by our measurements.

[71] *D. Swern*, in *D. Swern* (Ed.), "Organic Peroxides", Wiley Interscience, New York, Vol. **II**, 355–535 (1971).

[72] *D. D. Agarwal*, J. Mol. Catal. **44**, 65 (1988).

[73] *E. W. Garbisch, S. M. Schildcrout, D. B. Patterson* and *C. M. Sprecher*, J. Am. Chem. Soc. **87**, 2932 (1965).

[74] *H. Rickborn* and *J. H. H. Cham*, J. Org. Chem. **32**, 3576 (1967).

[75] *J. C. M. Bax* and *A. W. van der Made*, Unpublished MM2 force-field calculations.

[76] In separate experiments, we found that, at low concentration ($0.05\ mol \cdot dm^{-3}$), benzoic acid has no enhancing effect on the rate of epoxidation.

[77] Co-oxidation of aldehydes and alkenes by oxygen to carboxylic acids and epoxides, respectively, catalyzed by Co^{II}TP**P** or Mn^{III}(TP**P**)Cl has been described in [*T. Mlodnicka*, J. Mol. Catal. **36**, 205 (1986) and Refs. cited]. Co-oxidation is explained by a mechanism involving $RCO^{\bullet}$ and $RCOOO^{\bullet}$ radicals. The acylperoxy radicals are stated to be able to generate a manganese(V)–oxo complex which then acts as an epoxidation agent. We have several lines of evidence arguing against this mechanism from being operative in our system: *(i)* ketones lacking the carbonyl H are as aldehydes, *(ii)* the presence of oxygen is not required in our system, *(iii)* the proposed peracids would be very soluble ion the basic aqueous phase, and *(iv)* aldehydes and ketones act catalytically and not stoichiometrically in our model.

[78] *R. W. Murray* and *R. Yeyamaran*, J. Org. Chem. **50**, 2847 (1985).

[79] Since in the presence of 4-methylpyridine the reaction is highly stereospecific (*cis*/*trans* ratio 95:5) because of steric effects (see Ref. 20), measurements were made in the absence of 4-methylpyridine.

[80] Recently *Bruice* et al. published data which were said to "cast considerable doubt on previous (*i.e.*, our) interpretations of the kinetics of the CH_2Cl_2/H_2O biphasic system" [see Ref. 40 and *R. W. Lee, P. C. Nakagaki* and *T. C. Bruice*, J. Am. Chem. Soc. **111**, 1368 (1989)]. We would like to comment on these articles:

(i) The system studied by *Bruice* et al. differs from our system in: *(a)* the pH (LiOCl = 10 *versus* NaOCl = 13.5) and *(b)* the axial ligand (NAcPhIm *versus* pyridine). As we have shown, both factors exert such a profound influence on the kinetics that it is difficult to draw general conclusions from a specific experiment. For example, *Bruice* et al. noted that the transfer of OCl^- is rate-determining (a similar observation is reported in Ref. 29). This is explained by the facts that a lower pH, an imidazole-based ligand, and a reactive substrate increase the rate of formation of the active species to such an extent that another step (*i.e.*, the transportation of OCl^-) becomes rate-limiting. Under our standard conditions, starvation of the organic layer for hypochlorite is excluded.

(ii) Our kinetic scheme was discarded by *Bruice* et al. on the basis of a computer simulation of a version different from our model: dimerization was treated as an irreversible reaction, in contrast to our scheme in which dimerization is reversible.

(iii) *Bruice* et al. postulate a comproportionation of $[T_{2,4,6}$triMe**PP**$)MnO]^+$ with $Mn^{III}(T_{2,4,6}$triMe**PP**$)X$ to give two molecules of $Mn^{IV}(T_{2,4,6}$triMe**PP**$)X$ to fit the experimental data. The fate of the oxygen atom, however, is not specified as it is in the case of dimerization. For the sterically hindered ($T_{2,4,6}$triMe**PP**) ligand, we could not find this comproportionation reaction, as was shown in a low-temperature UV/Vis experiment in which 1 eqv. of $Mn^{III}(T_{2,4,6}$triMe**PP**$)X$ was added to a preformed solution of ($T_{2,4,6}$triMe**PP**)MnOCl. No decrease of the Mn^{III} absorption and increase of the 422 nm absorption could be noted.

[81] *S. C. Chakrabarthy*, in *W. S. Trahanowsky* (Ed.) "Oxidation in Organic Chemistry", Academic Press, New York, Part **C**, 343 (1978).

[82] *H. E. Fonouni, S. Krishnan, D. G. Kuhn* and *G. A. Hamilton*, J. Am. Chem. Soc. **105**, 7672 (1983).

[83] *R. R. Gagné, C. A. Koval* and *G. C. Lisensky*, Inorg. Chem. **19**, 2855 (1980).

[84] *H. Koepp, H. Wendt* and *H. Strehlow*, Z. Elektrochem. 483 (1960).

[85] *J. B. Kim, J. J. Leonard* and *F. R. Longo*, J. Am. Chem. Soc. **94**, 3986 (1972).

[86] *A. D. Adler, F. R. Longo, J. D. Finarelli, J. Goldmacher, J. Assour* and *L. Korsakoff*, J. Org. Chem. **32**, 476 (1967).

[87] *A. S. Semeikin, O. I. Koifman* and *B. D. Berezin*, Khim. Geterosikl. Soedin **10**, 1354 (1982), cited by *A. Bettelheim, B. A. White, S. A. Raybuck* and *R. W. Murray*, Inorg.Chem. **26**, 1009 (1987).

[88] *A. W. van der Made, E. J. H. Hoppenbrouwer, R. J. M. Nolte* and *W. Drenth*, Recl. Trav. Chim. Pays-Bas **107**, 15 (1988).

[89] *R. G. Little, J. A. Anton, P. A. Loach* and *J. A. Ibers*, J. Heterocycl. Chem. **12**, 343 (1975).